The Journal of Experimental Biology 215, 29-43
© 2012. Published by The Company of Biologists Ltd
doi:10.1242/jeb.061481

## RESEARCH ARTICLE

# Interactive effects of salinity and elevated $CO_2$ levels on juvenile eastern oysters, *Crassostrea virginica*

Gary H. Dickinson[1,*], Anna V. Ivanina[2,*], Omera B. Matoo[2], Hans O. Pörtner[3], Gisela Lannig[3], Christian Bock[3], Elia Beniash[1] and Inna M. Sokolova[2,†]

[1]Department of Oral Biology, University of Pittsburgh, 589 Salk Hall, 3501 Terrace Street, Pittsburgh, PA 15261, USA, [2]Department of Biology, University of North Carolina at Charlotte, 9201 University City Blvd, Charlotte, NC 28223, USA and [3]Integrative Ecophysiology, Alfred Wegener Institute for Polar and Marine Research in the Hermann von Helmholtz Association of National Research Centers e.V. (HGF), Am Handelshafen 12, 27570 Bremerhaven, Germany

*These authors contributed equally to this work
†Author for correspondence (isokolov@uncc.edu)

Accepted 4 October 2011

## SUMMARY

**Rising levels of atmospheric $CO_2$ lead to acidification of the ocean and alter seawater carbonate chemistry, which can negatively impact calcifying organisms, including mollusks. In estuaries, exposure to elevated $CO_2$ levels often co-occurs with other stressors, such as reduced salinity, which enhances the acidification trend, affects ion and acid–base regulation of estuarine calcifiers and modifies their response to ocean acidification. We studied the interactive effects of salinity and partial pressure of $CO_2$ ($P_{CO_2}$) on biomineralization and energy homeostasis in juveniles of the eastern oyster, *Crassostrea virginica*, a common estuarine bivalve. Juveniles were exposed for 11 weeks to one of two environmentally relevant salinities (30 or 15 PSU) either at current atmospheric $P_{CO_2}$ (~400 μatm, normocapnia) or $P_{CO_2}$ projected by moderate IPCC scenarios for the year 2100 (~700–800 μatm, hypercapnia). Exposure of the juvenile oysters to elevated $P_{CO_2}$ and/or low salinity led to a significant increase in mortality, reduction of tissue energy stores (glycogen and lipid) and negative soft tissue growth, indicating energy deficiency. Interestingly, tissue ATP levels were not affected by exposure to changing salinity and $P_{CO_2}$, suggesting that juvenile oysters maintain their cellular energy status at the expense of lipid and glycogen stores. At the same time, no compensatory upregulation of carbonic anhydrase activity was found under the conditions of low salinity and high $P_{CO_2}$. Metabolic profiling using magnetic resonance spectroscopy revealed altered metabolite status following low salinity exposure; specifically, acetate levels were lower in hypercapnic than in normocapnic individuals at low salinity. Combined exposure to hypercapnia and low salinity negatively affected mechanical properties of shells of the juveniles, resulting in reduced hardness and fracture resistance. Thus, our data suggest that the combined effects of elevated $P_{CO_2}$ and fluctuating salinity may jeopardize the survival of eastern oysters because of weakening of their shells and increased energy consumption.**

Key words: hypercapnia, ocean acidification, salinity, calcification, shell mechanical properties, energy status, mollusks, $^1$H-NMR spectroscopy.

## INTRODUCTION

Ocean acidification associated with increasing atmospheric $CO_2$ levels is an urgent problem in the present and future state of oceans. An increase in dissolved $CO_2$ reduces seawater pH and alters its carbonate chemistry. These changes affect multiple biological processes that depend on pH and/or the levels and speciation of inorganic carbon in seawater, such as photosynthetic carbon fixation and $CaCO_3$ deposition *via* biomineralization (Doney et al., 2009). Estuaries and coastal habitats, which are hotspots for biological diversity in the oceans, are likely to be strongly affected by an increase in atmospheric $CO_2$. Although the chemistry and hydrodynamics of estuarine waters are complex and highly variable, the long-term trend of seawater pH in certain estuarine systems correlates with the respective trends in the open ocean, suggesting that estuaries will also experience effects of ocean acidification. For example, mean seawater pH in polyhaline sites [>18 practical salinity units (PSU)] of the Chesapeake Bay decreased by 0.012 and 0.006 units year$^{-1}$ (in spring and summer, respectively) over the past 25 years (Waldbusser et al., 2011), a rate above the 50-year trend for the surface waters in the open ocean (–0.0019 units year$^{-1}$) (Doney et al., 2009). Moreover, brackish waters can experience large fluctuations in seawater pH and carbonate chemistry because of a lower buffering capacity (compared with open ocean waters with higher salinity), acidic inputs from land-based sources, and biological $CO_2$ production (Pritchard, 1967; Burnett, 1997; Ringwood and Keppler, 2002). In fact, the seawater dilution in estuaries exacerbates the acidification trend induced by elevated $CO_2$ (Denman et al., 2011). Because of this natural variability of seawater pH in estuaries, estuarine organisms are often considered to be more tolerant of pH fluctuations and ocean acidification than their open ocean counterparts. However, the effects of high partial pressure of $CO_2$ ($P_{CO_2}$) and low pH on estuarine organisms and their tolerance limits in the face of ocean acidification are not yet fully understood.

Marine calcifying organisms (such as mollusks, echinoderms and corals) that build calcium carbonate ($CaCO_3$) skeletons are susceptible to changes in seawater carbonate chemistry because both biomineralization and $CaCO_3$ dissolution can be directly affected by reduced pH and the degree of saturation for $CaCO_3$ (Kleypas et

al., 2006). Moreover, biomineralization is a complex, biologically regulated process that requires energy (Digby, 1968; Palmer, 1983; Palmer, 1992; Wheeler, 1992; Day et al., 2000; Furuhashi et al., 2009). Susceptibility to ocean acidification varies among marine calcifiers, although most studied species show reduced biomineralization rates in response to elevated $P_{CO_2}$ (Doney et al., 2009). In acidified seawater, an increase in energy consumption required for carbonate sequestration and mineral deposition may incur a significant energy cost to marine calcifiers (Palmer, 1983; Geller, 1990; Palmer, 1992; Day et al., 2000; Wood et al., 2008; Wood et al., 2010). Ocean acidification can also affect energy metabolism of marine organisms either directly, *via* metabolic effects of changing intracellular pH, and/or indirectly *via* the elevated energy demands for acid–base and ion homeostasis (Pörtner, 1987; Lannig et al., 2010; Pörtner, 2010). This may result in trade-offs of limited energy resources between different biological processes, including homeostasis, growth, reproduction, development and biomineralization (Sokolova et al., 2011). The metabolic response to ocean acidification is variable and depends on the species, degree of acidification and other environmental factors [see Pörtner and Bock, Beniash et al. and Lannig et al., and references therein (Pörtner and Bock, 2000; Beniash et al., 2010; Lannig et al., 2010)].

In estuarine waters, $CO_2$-driven acidification commonly co-occurs with other stressors, including temperature, hypoxia and salinity, that can affect both biomineralization and energy metabolism. The potential interactions between hypercapnia and other environmental stressors are not well understood, but recent studies indicate that such interactions may be quite complex (Gazeau et al., 2007; Pörtner, 2008; Gooding et al., 2009; Ries et al., 2009; Byrne et al., 2010; Pörtner, 2010). For example, a moderate increase in temperature partially alleviated negative effects of low pH on biomineralization in the sea urchin *Heliocidaris erythrogramma* and the oyster *Crassostrea virginica* (Byrne et al., 2010; Waldbusser et al., 2011), but not in the abalone *Haliotis coccoradiata*, while a more extreme warming led to inhibition of biomineralization in *H. erythrogramma* (Byrne et al., 2010). These results indicate species-specific and potentially non-linear effects of temperature and temperature–pH interactions. Environmental salinity is another factor that can affect seawater chemistry and modify responses to hypercapnia and low pH in estuarine organisms. Brackish waters have lower alkalinity and less buffering capacity compared with open ocean waters, leading to lower pH of the brackish waters both in normocapnia and under the elevated $P_{CO_2}$ conditions (Mook and Koene, 1975; Hofmann et al., 2009). Low salinity also results in major changes in water chemistry, such as reduced $Ca^{2+}$ concentrations and total inorganic carbon (Mook and Koene, 1975; Hofmann et al., 2009), which – in conjunction with changes in alkalinity, buffering capacity and pH – may affect metabolism and biomineralization in marine calcifiers. Both salinity and pH can strongly affect energy metabolism as well as ion and acid–base homeostasis (Kinne, 1971; Ballantyne and Moyes, 1987a; Truchot, 1988; Hawkins and Hilbish, 1992; Lannig et al., 2010), thus creating a physiological basis for the interactive effects of these stressors on estuarine organisms. The combined effects of hypercapnia and salinity on metabolic physiology and biomineralization of estuarine organisms, however, are not well understood and require further investigation.

Eastern oysters, *Crassostrea virginica* Gmelin 1791, are common bivalves in West Atlantic estuaries. They build thick, predominantly calcitic shells used for protection against predators and environmental stressors such as extreme salinity or pollutants (Davenport, 1985; Kennedy et al., 1996; Checa et al., 2007; Checa et al., 2009). Like other estuarine invertebrates, oysters can experience wide fluctuations of salinity, $P_{CO_2}$ and pH in their natural habitats, and these natural pH fluctuations may be further compounded by future ocean acidification. Oysters have a low capacity to compensate for disturbances in ion and acid–base status induced by changes in seawater pH and/or salinity, and their metabolism is sensitive to disturbances in extracellular and intracellular pH (Crenshaw, 1972; Pörtner, 2008). Mollusks, including oysters, are also osmoconformers, and therefore changes in environmental salinity directly translate into changes in intracellular osmolarity (Kinne, 1971; Prosser, 1973; Berger, 1986; Berger and Kharazova, 1997). Thus, salinity and pH stress, alone and in combination, can strongly affect metabolism and biomineralization in these organisms.

The goal of this study was to assess the combined effects of salinity (15–30) and $P_{CO_2}$ (400–800 μatm) on biomineralization, energy homeostasis and metabolite profile of juvenile *C. virginica*. Survival, body size, biomineralization-related parameters [shell mass and mechanical properties, and activity and mRNA expression of carbonic anhydrase (CA)], parameters of energy status (high-energy phosphates and tissue energy stores) as well as concentrations of anaerobic end products (alanine, acetate and succinate) and free amino acids were determined in oyster juveniles after 11 weeks exposure to different salinity and $P_{CO_2}$ levels.

## MATERIALS AND METHODS

### Chemicals

Unless otherwise indicated, all chemicals and enzymes were purchased from Sigma Aldrich (St Louis, MO, USA), Roche (Indianapolis, IN, USA) or Fisher Scientific (Pittsburg, PA, USA) and were of analytical grade or higher.

### Experimental design

The effects of two factors were assessed in this study: salinity and $P_{CO_2}$. Experiments were carried out at two salinity levels, 30 (high salinity) and 15 (low salinity), and two $P_{CO_2}$ levels, ~400 μatm (normocapnia) and ~700–800 μatm (hypercapnia), yielding four treatment groups. The salinity conditions were within the environmentally relevant range for this species, and the two selected $P_{CO_2}$ levels were representative of the present-day conditions (~400 μatm $CO_2$) and atmospheric $P_{CO_2}$ predicted by the moderate scenarios of the Intergovernmental Panel for Climate Change (IPCC 2007) for the year 2100 (~700–800 μatm $CO_2$). Oysters were randomly assigned to one of these four treatment groups. The group exposed to a salinity of 30 and a $P_{CO_2}$ of ~400 μatm was considered the control, as these conditions were close to the natural habitat conditions of the studied population. Non-reproductive juveniles were used in this study in order to avoid complications due to the varying energy demands of reproducing organisms in different stages of their reproductive cycle.

### Animal collection and maintenance

Juvenile oysters (7 weeks post-metamorphosis) were obtained from a local oyster supplier (J & B Aquafood, Jacksonville, NC, USA) and pre-acclimated for 5–7 days at 20°C and a salinity of 30 in recirculating water tanks with artificial seawater (ASW) (Instant Ocean®, Kent Marine, Acworth, GA, USA) prior to experimentation. Salinity was maintained at 30 for high salinity treatments and gradually lowered by approximately 2 PSU day$^{-1}$ to reach a salinity of 15 in the low salinity treatments. Once this was completed, oyster shells were stained with calcein {2,4-bis-[N,N′-di(carbomethyl)-aminomethyl]-fluorescein} to create an artificial growth mark to distinguish new shell growth. Calcein is incorporated into growing

$CaCO_3$ structures, creating a growth mark that brightly fluoresces upon excitation (Heilmayer et al., 2005; Riascos et al., 2007; Kaehler and McQuaid, 1999). Animals were incubated for 12 h in gently aerated ASW containing 50 mg $l^{-1}$ calcein. Calcein staining was conducted in normocapnia at the two respective salinities, and pH of the calcein solution in ASW was adjusted to 8.3 using Seachem Marine Buffer (Seachem, Madison, GA, USA). After calcein staining, oyster juveniles were rinsed with clean ASW and placed in the experimental incubation tanks.

For hypercapnic treatments, the seawater was bubbled with $CO_2$-enriched air (certified gas mixtures containing 21% $O_2$, 0.08% $CO_2$ and balance $N_2$; Roberts Oxygen, Charlotte, NC, USA), whereas the normocapnic treatments were bubbled with ambient air. The gas flow rates were adjusted in such a way that further increase in the bubbling rate did not lead to a change in seawater pH, indicating that our systems were in a steady state. Salinity was determined using a YSI30 salinity, temperature and conductivity meter (YSI Inc., Yellow Springs, OH, USA). Water temperature was maintained at 21±1°C in all tanks and salinity either at 30±0.5 or 15±0.5. Water was changed every other day using ASW pre-equilibrated with the respective gas mixtures. Artificial seawater was prepared from the same batch of Instant Ocean® sea salt throughout the experiment to minimize variations in pH, alkalinity and ionic composition. A single batch of seawater was prepared during every water change and used for all experimental treatments; seawater with a salinity of 15 was prepared from seawater at a salinity of 30 by dilution. The experimental incubations of juvenile oysters lasted 11 weeks.

During the preliminary acclimation and experimental incubations, oysters were fed *ad libitum* every other day with a commercial algal blend (5 ml per 30 l tank) containing *Nannochloropsis oculata*, *Phaeodactylum tricornutum* and *Chlorella* sp. with a cell size of 2–20 μm (DT's Live Marine Phytoplankton, Sycamore, IL, USA). Algae were added to the tanks following each water change. Experimental tanks were checked for mortality daily, and oysters that gaped and did not respond to a mechanical stimulus were recorded as dead and immediately removed.

### Seawater chemistry

Carbonate chemistry of seawater was determined as described in an earlier study (Beniash et al., 2010). Briefly, samples were periodically collected from experimental tanks during the 11 weeks of exposure, placed in air-tight containers without air space, stabilized by mercuric chloride poisoning (Dickson et al., 2007) and kept at +4°C until further analysis. Water pH was measured at the time of collection using a pH electrode (pH meter Model 1671 equipped with a 600P pH electrode, Jenco Instruments, San Diego, CA, USA) calibrated with National Institute of Standards and Technology standard pH buffer solutions (National Bureau of Standards, NBS standards) (Fisher Scientific). Water temperature and salinity were recorded at the same time. Total dissolved inorganic carbon (DIC) concentrations were measured within a week of collection by Nutrient Analytical Services (Chesapeake Biological Laboratory, Solomons, MD, USA). DIC was determined using a Shimadzu TOC5000 gas analyzer equipped with a non-dispersive infrared sensor detector for $CO_2$ determination (Shimadzu Scientific Instruments, Columbia, MD, USA) calibrated with DIC standards (Nacalai Tesque, Columbia, MD, USA) recommended by and purchased from the instrument's manufacturer. Samples were measured immediately after opening to minimize gas exchange. Three to five replicates were run for each sample, and precision of the analysis was 1% or better for the technical replicates from the same sample. Temperature, salinity and pH were measured at the time of collection and, along with the total DIC levels, were used to calculate $P_{CO_2}$, alkalinity and the saturation state (Ω) for calcite and aragonite in seawater using co2sys software (Lewis and Wallace, 1998). For co2sys settings, we used the NBS scale of seawater pH constants from Millero et al. (Millero et al., 2006), the $KSO_4^-$ constant from Dickson et al. [(Dickson et al., 1990) cited in Lewis and Wallace (Lewis and Wallace, 1998)], and concentrations of silicate and phosphate for Instant Ocean® seawater (silicate: 0.17 and 0.085 μmol $kg^{-1}$ at salinities of 30 and 15, respectively, and phosphate: 0.04 and 0.02 μmol $kg^{-1}$ at salinities of 30 and 15, respectively). Water chemistry data for these samples are given in Table 1. It is worth noting that pH and carbonate chemistry differed between salinities of 30 and 15 at the same $P_{CO_2}$ levels, reflecting changes in the DIC, buffering capacity and alkalinity associated with dilution of seawater; this situation mimics conditions naturally occurring in brackish estuarine waters where seawater and freshwater mix (Mook and Koene, 1975; Hofmann et al., 2009). In addition, total alkalinity of Instant Ocean® seawater is slightly higher (~3000 μmol $kg^{-1}$ ASW in the high salinity treatment) than values reported from the natural seawater (~2300–2500 μmol $kg^{-1}$ seawater) (Zeebe and Wolf-Gladrow, 2001; Riebesell et al., 2010), as is typical for artificial sea salt formulations. Thus, the estimates of the effects

Table 1. Summary of water chemistry parameters during experimental exposures of juvenile eastern oysters, *Crassostrea virginica*

| | Exposure salinity | | | |
|---|---|---|---|---|
| | 15 | | 30 | |
| Parameter | Normocapnia | Hypercapnia | Normocapnia | Hypercapnia |
| pH | 8.11±0.09 | 7.97±0.03 | 8.36±0.04 | 8.1+0.01 |
| Temperature (°C) | 22.6±0.8 | 22.2+0.8 | 21.4±0.7 | 21.4+0 |
| Salinity | 15.1±0.2 | 15.2±0.3 | 30.1±0.1 | 30+0 |
| $P_{CO_2}$ (μatm) | 470.4±160.1 | 676.5±65.7 | 392.1±30.0 | 802.3±3.6 |
| Total alkalinity (μmol $kg^{-1}$ SW) | 1628.0±163.5 | 1734.8±100.2 | 3512.3±224.2 | 3546.7±15. 7 |
| DIC (μmol $kg^{-1}$ SW) | 1549.9±171.1 | 1683.2±96.8 | 3058.5±171.7 | 3287.3±14.8 |
| $HCO_3^-$ (μmol $kg^{-1}$ SW) | 1462.9±167.7 | 1602.7±91.3 | 2678.0±127.1 | 3035.2±13.6 |
| $CO_3^{2-}$ (μmol $kg^{-1}$ SW) | 70.5±8.6 | 56.6±4.8 | 367.6±47.7 | 225.4±1.0 |
| $CO_2$ (μmol $kg^{-1}$ SW) | 16.5±5.2 | 23.9±1.8 | 12.9±0.8 | 26.6±0.1 |
| Ω Ca | 1.94±0.23 | 1.56±0.14 | 9.09±1.18 | 5.58±0.03 |
| Ω Arg | 1.16±0.14 | 0.93±0.08 | 5.85±0.76 | 3.58±0.02 |

Salinity, temperature, pH and dissolved inorganic carbon (DIC) were determined in samples from experimental tanks at the beginning, middle and end of experimental exposures as described in the Materials and methods. Other parameters were calculated using co2sys software. Data are presented as means ± s.d. *N*=6 for the hypercapnic group at a salinity of 30 and *N*=11–12 for all other exposures. SW, seawater.

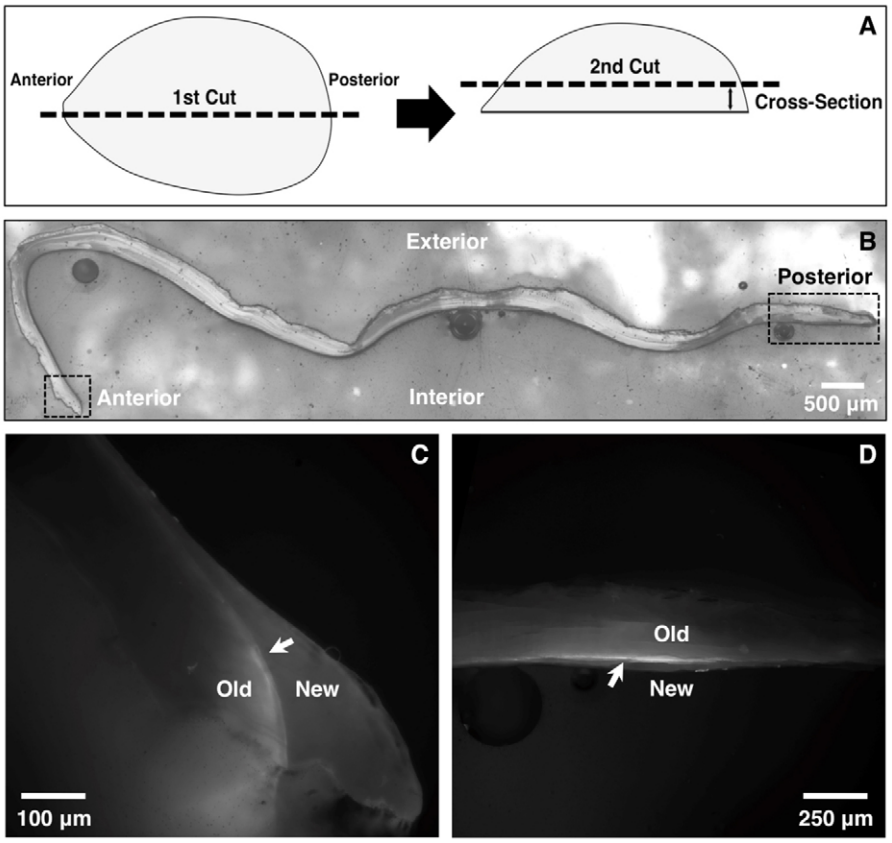


Fig. 1. Preparation of juvenile oyster samples for mechanical testing, and identification of new shell grown during experimental exposure. (A) Embedded left shell valves were first cut longitudinally, from anterior to posterior, along their longest axis. A second cut was made parallel to the first to produce a 1–3 mm thick section. (B) Full cross-section of a juvenile shell under polarized light. New growth was observed at the far anterior and posterior ends of the shell. (C,D) Epifluorescence (FITC channel) micrographs of the anterior (C) and posterior (D) of the shell. Fluorescence micrographs correspond to regions denoted by boxes in B. Calcein staining appears as a distinct line, as indicated by arrows.

of ocean acidification obtained in the present study are conservative, as the $CO_2$-induced changes in pH and carbonate chemistry will be stronger in the natural seawater with lower alkalinity. Oxygen levels in experimental tanks were tested using Clark-type oxygen probes (YSI 5331 oxygen probe, YSI Inc.) connected to a YSI 5300A biological oxygen monitor and were >95% of air saturation throughout all exposures.

### Shell and soft tissue mass measurements

Following experimental exposure, approximately 50 oysters from each treatment group were stored in 70% ethanol and shipped to the University of Pittsburgh for mass measurements and mechanical testing. In addition to the four treatment groups, a set of 50 oysters that had been preserved in 70% ethanol prior to experimental exposures was also included in the shipment. These oysters are referred to as the time zero group. Only oysters with intact shells were considered in further analyses.

For mass measurements, 25 individuals were randomly selected from each treatment group, briefly rinsed in deionized water (DI), air-dried for 5 days and lyophilized for approximately 16 h. Lyophilized oysters were individually weighed on a microbalance (Metler-Toledo XP 26, Columbus, OH, USA) with precision of 0.01 mg or better to obtain each oyster's total mass. To remove soft tissue, oysters were incubated in sodium hypochlorite (NaOCl; commercial Clorox diluted to obtain 2% v/v NaOCl and filtered through a 0.2 µm filter) on an orbital shaker at 250 rpm at room temperature until all soft tissue was removed. Shells were sonicated, rinsed several times in DI, air-dried at room temperature for 3 days and finally lyophilized for approximately 16 h. Lyophilized shells were weighed to determine shell mass, and soft tissue dry mass was determined for each individual by subtracting shell mass from total mass.

### Micromechanical testing of shells

Micromechanical testing was conducted on seven shells from each treatment group. A similar distribution of shell masses was chosen for each group. Left (bottom) shell valves were used for mechanical testing, as the region of new growth during experimental exposure was most distinct in these valves. Left shell valves were mounted in epoxy resin (Epofix, ESM, Hatfield, PA, USA) and polymerized for 24 h at room temperature. Embedded shells were cut longitudinally, transecting the acute apical tip (anterior) to the most distal edge (posterior), using a slow-speed water-cooled diamond saw (IsoMet, Buehler, Lake Bluff, IL, USA), as depicted in Fig. 1A. A second cut was made parallel to the first to produce a 1- to 3-mm-thick section. Sections were ground and then polished with Metadi diamond suspensions at 6, 1 and 0.25 µm diamond particle size on a grinder-polisher (MiniMet 1000, Buehler). Grinding and polishing was conducted using a saturated $CaCO_3$ solution (pH 7.8). A saturated $CaCO_3$ solution was prepared by mixing calcium and carbonate salts at very high concentrations and letting the mineral precipitate over several hours. The mixture was centrifuged and the supernatant was used to polish the samples. No etching of the shell samples was observed during grinding or polishing.

After polishing, the region of new shell growth formed during the experimental exposures was identified based on the calcein growth mark, as shown in Fig. 1B–D. Imaging was conducted on a fluorescence microscope in the fluorescein isothiocyanate channel (Nikon TE2000, Melville, NY, USA). Although calcein staining was observed at both the anterior and posterior ends of the shell cross-sections, staining was most distinct in the anterior end, which was chosen for the microindentation testing (Fig. 1C,D). Dimensions of the new growth region for each shell were determined from a digital micrograph using microscopy software (NIS Elements ver.

3.20.01, Melville, NY, USA), which enabled identification of the new growth region during hardness testing.

Vickers microhardness tests were carried out using a microindentation hardness tester (IndentaMet 1104, Buehler) on polished shells at a load of 0.245 N and a dwelling time of 5 s. Three to six indentations per shell were made, depending on the size of the new growth region. All indents were made at least 30 μm away from the new growth region. Vickers microhardness values were averaged for each shell sample. Digital photographs were taken before and immediately after each indentation. This enabled quantification of the longest crack produced by each indent, which was measured using Adobe Photoshop (ver. 4.0, San Jose, CA, USA) as the radius of a circle radiating from the center of the indent and enclosing all visible cracks. The crack radius for a shell sample was obtained by averaging the crack radii for all indents on that sample, expressed in μm. In this study, we chose to use mean crack radius as a proxy for fracture toughness ($K_c$). There are a number of empirical equations used to calculate toughness from the length of cracks generated by microindentation (Anstis et al., 1981; Baldassarri et al., 2008); however, because the empirical constants used in these equations were not determined for oyster shells, we chose to use the crack length as a proxy for $K_c$. The term 'fracture resistance' is used in the text in place of $K_c$ to avoid confusion.

Representative indents were imaged by scanning electron microscopy (SEM) in the back-scattered electron mode. Embedded and polished shell cross-sections (Fig. 1A,B) were carbon coated and imaged on a field emission SEM (JSM-6330F, Jeol, Peabody, MA, USA) at 10 kV with a working distance of 12.5–15.2 mm in the ×500 to ×3000 magnification range.

### Physiological and biochemical traits

A separate subset of experimental animals, which had not been preserved in ethanol, was used for analyses of tissue metabolite concentrations, enzyme activities and mRNA expression. For these analyses, oyster juveniles were shock-frozen in liquid nitrogen immediately after collection and stored in liquid nitrogen to prevent metabolite, protein and mRNA degradation.

### CA activity

The whole soft body of juveniles was homogenized in homogenization medium (1:10 w/v) containing 250 mmol l$^{-1}$ sucrose, 40 mmol l$^{-1}$ Tris-$H_2SO_4$ and 80 μg ml$^{-1}$ phenyl methane sulfonylfluoride (PMSF), pH 7.5 using a Kontes Duall® glass-glass homogenizer (Fisher Scientific). Homogenates were centrifuged for 10 min at 10,000 ***g*** at 4°C. The supernatant was collected and stored at –80°C until further analysis. A pilot study showed that freezing and thawing did not affect CA activity in oyster homogenates (data not shown).

CA activity was determined as acetazolamide (AZM)-sensitive esterase activity following a standard method modified from Gambhir et al. (Gambhir et al., 2007). The assay consisted of 100 μl of tissue homogenate in 1 ml of assay medium containing 63 mmol l$^{-1}$ Tris-$H_2SO_4$, pH 7.5 and 75 μmol l$^{-1}$ p-nitrophenyl acetate (p-NPA) as a substrate. Total esterase activity in the sample was measured as a change in absorbance at 348 nm using a Cary® 50 UV-Vis spectrophotometer (Varian Inc., Cary, NC, USA). The temperature of the assay mixture was maintained at 20±0.1°C using a water-jacketed cuvette holder (Varian Inc.). After determining the initial slope of esterase reaction, a specific CA inhibitor, AZM (7 mmol l$^{-1}$), was added to the assay, and CA activity was determined as the difference in the initial reaction slopes before and after AZM addition using the molar extinction coefficient for p-nitrophenol of 51 mmol$^{-1}$ cm$^{-1}$ at 348 nm and pH 7.5. The reaction was linear for the complete duration of the assay (10–12 min). This assay allows measurement of CA activity at physiologically relevant temperatures in contrast to hydratase activity assays [such as a pH-stat Wilbur–Anderson method (Wilbur and Anderson, 1948) and its modifications)] carried out at non-physiologically low temperatures (approximately 0°C) to prevent rapid spontaneous hydration of $CO_2$ (Nielsen and Frieden, 1972; Smeda and Houston, 1979; Gambhir et al., 2007; Malheiro et al., 2009). CA activity determined with the AZM-sensitive esterase assay correlates with the cellular CA content (Gambhir et al., 2007). Protein concentration was measured in tissue homogenates of juvenile oysters using the Bio-Rad protein assay (Bio-Rad Laboratories, Hercules, CA, USA) using bovine serum albumin as a standard. Specific CA activity was expressed as U g$^{-1}$ protein, where 1 U corresponds to the amount of enzyme catalyzing the breakdown of 1 μmol p-NPA min$^{-1}$ at 20°C and pH 7.5.

### RNA extraction and quantitative real-time PCR

Total RNA was extracted from pooled whole-body tissues of 10–12 juveniles using Tri Reagent (Sigma-Aldrich) according to the manufacturer's protocol with a tissue to Tri reagent ratio of 1:10 (w/v) or less. Single-stranded cDNA was obtained from 5 μg total RNA using 200 U μl$^{-1}$ SuperScript III Reverse Transcriptase (Invitrogen, Carlsbad, CA, USA) and 50 μmol l$^{-1}$ of oligo(dT)$_{18}$ primers.

Transcript expression of CA mRNA was determined using quantitative real-time PCR (qRT-PCR) using a LightCycler® 2.0 Real Time PCR System (Roche) and QuantiTect SYBR Green PCR kit (Qiagen, Valencia, CA, USA) according to the manufacturers' instructions. Specific primers were designed to amplify cDNA using *C. virginica* CA, β-actin and 18S ribosomal RNA (rRNA) sequences. Gene sequences for *C. virginica* CA were obtained from the Marine Genomics database (www.marinegenomics.org, sequence accession number MGID94539); those for β-actin were obtained from GenBank (NCBI accession number X75894.1). For 18S rRNA, consensus primers were designed against highly conserved nucleotide sequences using 18S rRNA sequences from four bivalves: *C. virginica*, *Crassostrea gigas*, *Mytilus edulis* and *Mercenaria mercenaria* (NCBI accession numbers L78851.1, AB064942, L33448.1 and AF120559.1, respectively). Primer sequences were (5′ to 3′ orientation) as follows: for CA, forward CarbAnh-F23 AGA GGA ACA CCG TAT CGG AGC CA and reverse CarbAnh-R155 ATG TCA ATG GGC GAC TGC CG; for β-actin, forward Act-Cv-F437 CAC AGC CGC TTC CTC ATC CTC C and reverse Act-Cv-R571 CCG GCG GAT TCC ATA CCA AGG; and for 18s rRNA, forward 18sRNA GGT AAC GGG GAA TCA GGG TTC GAT and reverse 18sRNA TGT TAT TTT TCG TCA CTA CCT CCC CGT.

Briefly, the qRT-PCR reaction mixture consisted of 5 μl of 2× QuantiTect SYBR Green master mix, 0.3 μmol l$^{-1}$ of each forward and reverse gene-specific primers, 1 μl of 10× diluted cDNA template and water to adjust to 10 μl. The reaction mixture was subjected to the following cycling: 15 min at 95°C to denature DNA and activate *Taq* polymerase and 50 cycles of 15 s at 94°C, 20 s at 55°C and 15 s at 72°C. SYBR Green fluorescence (acquisition wavelength 530 nm) was measured at the end of each cycle for 2 s at the read temperature of 78°C (to melt all primer dimers but not the amplified gene product). Serial dilutions of a cDNA standard were amplified in each run to determine amplification efficiency (Pfaffl, 2001). A single cDNA sample from gills of an adult *C. virginica* was used as an internal cDNA standard and included in each run to test for run-to-run amplification variability. The CA mRNA expression was standardized relative to β-actin mRNA or 18S rRNA and against the internal

standard as described elsewhere (Pfaffl, 2001; Sanni et al., 2008). The qualitative CA mRNA expression patterns were similar regardless of whether β-actin or 18S rRNA mRNA was used for normalization. However, β-actin mRNA levels were less variable between exposure conditions than 18S rRNA transcripts. Salinity had a significant effect on 18S rRNA levels (ANOVA, $P$=0.009) but not on β-actin mRNA (ANOVA, $P$=0.649), whereas $P_{CO_2}$ of exposure did not significantly affect mRNA levels for β-actin or 18S rRNA (ANOVA, $P$=0.868–0.938). Therefore, we report the data on CA mRNA expression standardized to β-actin mRNA.

### Biochemical analyses of juvenile tissues

Whole-body tissues of 10–12 juveniles were pooled and immediately shock-frozen in liquid nitrogen. Frozen tissues were powdered with a mortar and pestle under liquid nitrogen and extracted using ice-cold 0.6 mol l$^{-1}$ perchloric acid (PCA) as described elsewhere (Sokolova et al., 2000). Neutralized, deproteinized PCA extracts were stored at –80°C and used for metabolic profiling using $^1$H-nuclear magnetic resonance (NMR) spectroscopy as well as to determine concentrations of adenylates and D-glucose using standard spectrophotometric NADH- or NADPH-linked enzymatic assays (Grieshaber et al., 1978; Bergmeyer, 1985). Briefly, the assay conditions were as follows: for ADP, 38.5 mmol l$^{-1}$ triethanolamine (TRA) buffer, pH 7.6, 0.04 mmol l$^{-1}$ NADP, 7 mmol l$^{-1}$ $MgCl_2\times6H_2O$, 50 mmol l$^{-1}$ glucose, 0.462 U ml$^{-1}$ glucose-6-phosphate dehydrogenase, 1.8 U ml$^{-1}$ hexokinase; for ADP and AMP, 58 mmol l$^{-1}$ TRA buffer, pH 7.6, 3 mmol l$^{-1}$ phoshoenolpyruvate, $MgSO_4\times7H_2O$ 6.2%, KCl 6.7%, 0.09 mmol l$^{-1}$ NADH, 24 U ml$^{-1}$ lactate dehydrogenase, 18 U ml$^{-1}$ pyruvate kinase, 16 U ml$^{-1}$ myokinase; and for D-glucose, 38.5 mmol l$^{-1}$ TRA buffer, pH 7.6, 0.04 mmol l$^{-1}$ NADP, 7 mmol l$^{-1}$ $MgCl_2\times6H_2O$, 0.462 U ml$^{-1}$ glucose-6-phosphate dehydrogenase, 1.8 U ml$^{-1}$ hexokinase.

Glycogen concentration was measured in PCA extracts after enzymatic hydrolysis of glycogen to D-glucose by glucoamylase (Keppler and Decker, 1984) and determined by the difference in the D-glucose levels in the tissue extract before and after glucoamylase treatment. Tissue lipid content was measured using a standard method of chloroform extraction (Folch et al., 1957; Iverson et al., 2001). Whole-body tissues of 10–12 juveniles (~50 mg wet mass) were homogenized in a chloroform/methanol mixture (2:1 v/v) using a tissue to chlorophorm/methanol ratio of 1:20 (w/v). Samples were sonicated for 1 min (output 69 W, Sonicator 3000, Misonix, Farmingdale, NY, USA), vortexed for 2 min and centrifuged for 5 min at 13,000 ***g***. The supernatant was transferred into a new tube and the chloroform/methanol extraction was repeated on the tissue pellet. The supernatants of two extractions were pooled, mixed with water (25% of the total volume of supernatant) and centrifuged for 5 min at 13,000 ***g***. The lower phase (chloroform) was transferred to a pre-weighed tube and the chloroform was evaporated to determine the mass of the extracted lipids.

For protein determination, whole bodies of 10–12 juveniles were homogenized in ice-cold homogenization buffer (100 mmol l$^{-1}$ Tris, pH 7.4, 100 mmol l$^{-1}$ NaCl, 1 mmol l$^{-1}$ EDTA, 1 mmol l$^{-1}$ EGTA, 1% Triton-X100, 10% glycerol, 0.1% sodium dodecylsulfate, 0.5% deoxycholate, 0.5 μg ml$^{-1}$ leupeptin, 0.7 μg ml$^{-1}$ pepstatin, 40 μg ml$^{-1}$ PMSF and 0.5 μg ml$^{-1}$ aprotinin) using hand-held Kontes Duall tissue grinders (Fisher Scientific). Homogenates were sonicated 3×10 s (output 69 W, Sonicator 3000, Misonix) to ensure complete release of the proteins, with cooling on ice (1 min) between sonications. Homogenates were centrifuged for 10 min at 20,000 ***g*** and 4°C, and supernatants were used for protein determination. Protein content was measured using the Bio-Rad Protein Assay kit according to the manufacturer's instructions (Bio-Rad Laboratories). Concentrations of glycogen, lipids and proteins were expressed in mg g$^{-1}$ wet tissue mass, and concentrations of adenylates and D-glucose in μmol g$^{-1}$ wet tissue mass.

### Metabolic profiling using $^1$H-NMR spectroscopy

Preparation of samples and NMR spectroscopy were performed as described by Lannig et al. (Lannig et al., 2010), with the following modifications. Freeze-dried PCA extracts were resolved in 500 μl $D_2O$ containing 1% trimethylsilyl propionate (TSP) as an internal reference and concentration standard for NMR spectroscopy. Fully relaxed 1D, one pulse $^1$H-NMR spectroscopy with F1 presaturation for water suppression was used for an analysis of metabolic profiles of the PCA extracts. All spectra were recorded with an inverse $^1$H-broad band probe ($^1$H/BBI) on a 400 MHz 9.4T WB NMR spectrometer with Avance electronics (Bruker Biospin GmbH, Silberstreifen, Germany). Prior to all NMR recordings, field homogeneity was optimized using TopShim (Bruker Biospin GmbH), resulting in typical line widths of 1 Hz. Acquisition parameters were as follows: pulse program zgpr, TD=32k, NS=32, DS=2, SW=6k, AQ=2726 s, D1=10 s, RG 181, flip angle 90 deg, presaturation level 60 dB, resulting scan time 7.12 min.

Post-processing of spectra was performed automatically using TopSpin 2.5 (Bruker Biospin GmbH). Briefly, all data were zero filled to 64k, processed with an exponential multiplication of 0.5 Hz and automated baseline and phase corrections. Quantification of signal areas was performed using a fit routine (mdcon, Bruker Biospin GmbH) and calculated relative to TSP as an internal reference standard. Specific metabolites were identified using chemical shift tables from Tikunov et al. (Tikunov et al., 2010) and as described in Lannig et al. (Lannig et al., 2010). After an operator-controlled screening of all spectra, only signals from metabolites displaying the most obvious changes were analyzed and quantified. Changes in metabolites of interest were expressed in percent change from the control group (maintained at a salinity of 30 and a $P_{CO_2}$ of ~400 μatm).

### Calculations and statistics

Cumulative mortality after 11 weeks was compared between the different treatment groups using a chi-square test. Effects of the factors salinity, $P_{CO_2}$ and their combination on physiological parameters and shell and body mass and material properties of the shells were assessed using generalized linear model ANOVA after testing for the normality of data distribution and homogeneity of variances. Both factors were treated as fixed and had two levels each (15 and 30 for salinity, and normocapnia and hypercapnia for $P_{CO_2}$). In the few cases where data distribution deviated from normality and/or variances were not homogenous, the data were log-transformed to ensure compliance with the ANOVA assumptions. *Post hoc* tests (Fisher's least square difference) were used to test the differences between the group means. Table 2 presents the results of ANOVA conducted on raw or log-transformed data as appropriate, but all means and standard errors are given for the raw (non-transformed) data. Sample sizes for all experimental groups were five to nine except for lipid content ($N$=4) and protein content of the juveniles maintained at ~400 μatm $P_{CO_2}$ and a salinity of 15, where $N$=3 due to sample loss. For shell and body mass, as well as for the mechanical properties of the shells, each sample represented an individual oyster. For all other endpoints, each sample consisted of the pooled tissues of 10–12 individual juveniles. Unless otherwise indicated, data are represented as means ± s.e.m. The differences were considered significant if the probability of Type I error was less than 0.05.

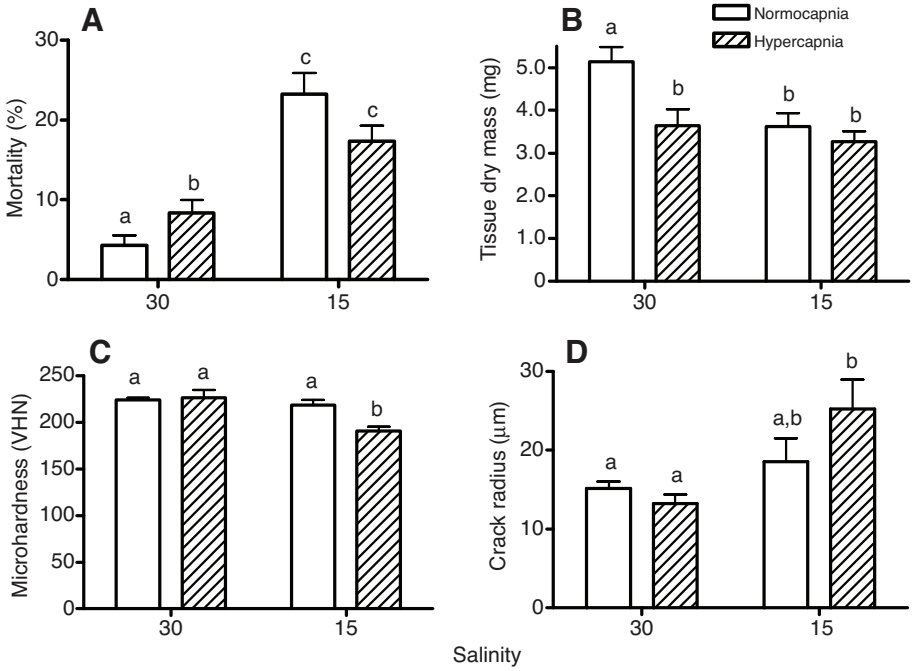


Fig. 2. Mortality, soft body mass and mechanical characteristics of the newly grown shell in juveniles of the eastern oyster *Crassostrea virginica* maintained for 11 weeks in different salinities and $P_{CO_2}$ levels. Exposure conditions are given in Table 1. (A) Cumulative mortality after 10 weeks exposure; (B) soft body mass; (C) microhardness of the newly grown shell expressed as Vickers microhardness number (VHM); (D) mean crack radius in response to a mechanical stress. Within each graph, different letters indicate means that are significantly different from each other ($P$<0.05). If the columns share a letter, the respective means are not significantly different ($P$>0.05).

## RESULTS

### Mortality

At a salinity of 30, elevated $P_{CO_2}$ significantly increased mortality of juvenile oysters by almost twofold compared with normocapnia ($P$<0.05; Fig. 2A). Low (15) salinity led to a fourfold to fivefold increase in juvenile mortality compared with the controls maintained in normocapnia and high salinity ($P$<0.05; Fig. 2A). However, no additional effect of elevated $P_{CO_2}$ on mortality of juveniles was observed at low salinity (Fig. 2A).

### Shell and body mass

Total body mass, shell mass and soft tissue mass did not significantly change during incubation under control conditions (ANOVA, $P$=0.23–0.58 for comparisons of the groups collected at time 0 and

Table 2. ANOVA results of the effects of exposure salinity, $P_{CO_2}$ and their interaction on shell and soft tissue mass, mechanical shell properties, enzyme activities and energy-related indices in juvenile *C. virginica*

| Parameter | Salinity | $P_{CO_2}$ | Salinity × $P_{CO_2}$ |
|---|---|---|---|
| Shell and body mass | | | |
| Total dry mass | $F_{1,116}$=1.29, $P$=0.258 | $F_{1,116}$=0.94, $P$=0.333 | $F_{1,119}$=0.42, $P$=0.519 |
| Shell mass | $F_{1,116}$=1.02, $P$=0.313 | $F_{1,116}$=0.71, $P$=0.400 | $F_{1,116}$=0.62, $P$=0.431 |
| Soft tissue dry mass | **$F_{1,116}$=6.73, $P$=0.011** | **$F_{1,116}$=6.33, $P$=0.013** | $F_{1,116}$=2.43, $P$=0.122 |
| Mechanical shell properties | | | |
| Vickers microhardness | **$F_{1,31}$=17.35, $P$=0.002** | **$F_{1,31}$=7.43, $P$=0.01** | **$F_{1,31}$=9.61, $P$=0.004** |
| Crack radius | **$F_{1,31}$=12.00, $P$=0.002** | $F_{1,31}$=0.65, $P$=0.427 | **$F_{1,116}$=4.43, $P$=0.044** |
| Enzyme activity and mRNA expression | | | |
| Carbonic anhydrase mRNA | $F_{1,22}$=1.62, $P$=0.217 | **$F_{1,22}$=5.24, $P$=0.032** | $F_{1,22}$=1.30, $P$=0.267 |
| Carbonic anhydrase activity | **$F_{1,21}$=9.27, $P$=0.006** | $F_{1,21}$=0.48, $P$=0.495 | $F_{1,21}$=3.42, $P$=0.078 |
| Esterase activity | **$F_{1,21}$=5.31, $P$=0.031** | $F_{1,21}$=0.69, $P$=0.414 | $F_{1,21}$=3.14, $P$=0.091 |
| Tissue metabolites | | | |
| ATP | $F_{1,23}$=1.03, $P$=0.321 | $F_{1,23}$=2.62, $P$=0.119 | $F_{1,23}$=0.37, $P$=0.546 |
| ADP | $F_{1,23}$=0.73, $P$=0.401 | **$F_{1,23}$=5.08, $P$=0.034** | $F_{1,23}$=2.59, $P$=0.121 |
| AMP | **$F_{1,23}$=7.94, $P$=0.010** | $F_{1,23}$=1.76, $P$=0.197 | $F_{1,23}$=1.06, $P$=0.314 |
| Σ adenylates | $F_{1,23}$=0.93, $P$=0.346 | $F_{1,23}$=3.24, $P$=0.085 | $F_{1,23}$=0.18, $P$=0.675 |
| ADP/ATP | $F_{1,23}$=2.82, $P$=0.106 | $F_{1,23}$=0.49, $P$=0.490 | $F_{1,23}$=2.23, $P$=0.149 |
| AEC | $F_{1,23}$=0.73, $P$=0.403 | $F_{1,23}$=0.05, $P$=0.823 | **$F_{1,23}$=4.29, $P$=0.049** |
| D-glucose | $F_{1,23}$=0.01, $P$=0.929 | $F_{1,23}$=0.34, $P$=0.562 | $F_{1,23}$=0.38, $P$=0.544 |
| Glycogen | $F_{1,23}$=0.07, $P$=0.791 | **$F_{1,23}$=6.15, $P$=0.021** | $F_{1,23}$=0.34, $P$=0.563 |
| Lipids | $F_{1,12}$=4.49, $P$=0.055 | $F_{1,23}$=4.47, $P$=0.056 | **$F_{1,23}$=5.68, $P$=0.034** |
| Proteins | $F_{1,22}$=1.48, $P$=0.237 | $F_{1,22}$=0.01, $P$=0.933 | $F_{1,22}$=0.37, $P$=0.552 |
| Betaine | **$F_{1,23}$=53.57, $P$<0.0001** | $F_{1,23}$=0.01, $P$=0.936 | $F_{1,23}$=0.00, $P$=0.994 |
| Lysine | **$F_{1,18}$=6.48, $P$=0.022** | $F_{1,18}$=0.05, $P$=0.823 | $F_{1,18}$=0.02, $P$=0.890 |
| Succinate | **$F_{1,22}$=8.55, $P$=0.008** | $F_{1,22}$=0.00, $P$=0.979 | $F_{1,22}$=0.03, $P$=0.872 |
| Acetate | **$F_{1,21}$=11.38, $P$=0.003** | **$F_{1,21}$=5.17, $P$=0.035** | **$F_{1,21}$=4.78, $P$=0.042** |
| Alanine | **$F_{1,21}$=8.58, $P$=0.009** | $F_{1,21}$=0.17, $P$=0.687 | $F_{1,21}$=0.44, $P$=0.516 |

*F*-values are given with degrees of freedom for the factor and the error in subscript. Significant values ($P$<0.05) are highlighted in bold.
AEC, adenylate energy change.

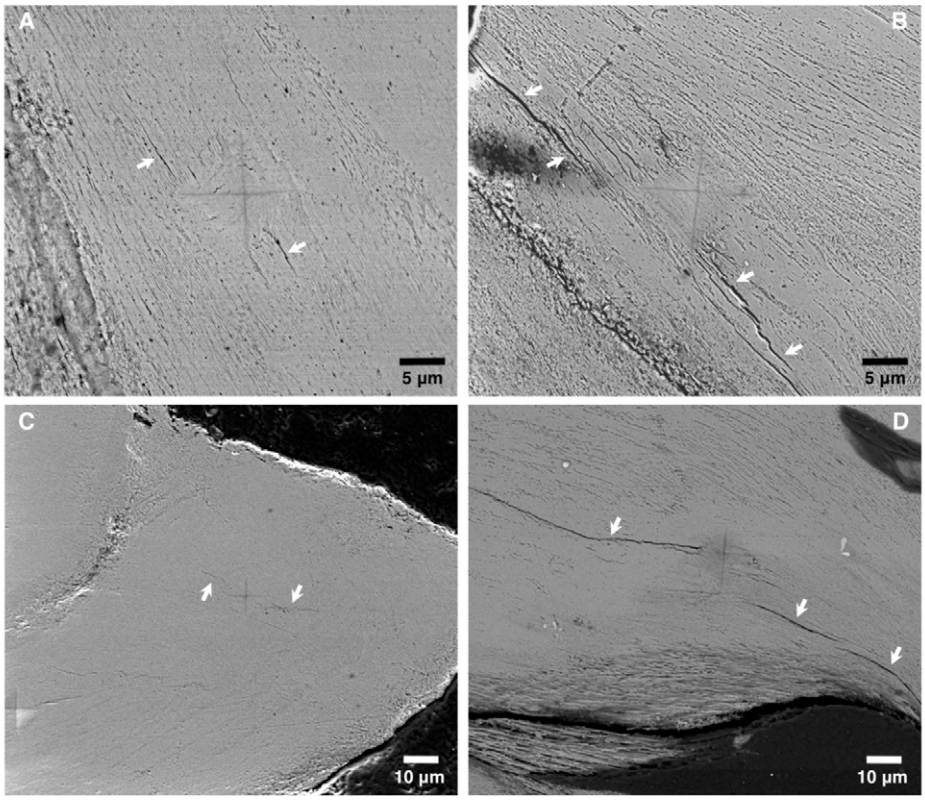


Fig. 3. Back-scattered SEM micrographs of shells from control juveniles (maintained under normocapnic conditions at a salinity of 30) (A,C) and shells from juveniles maintained under hypercapnia at a low salinity of 15 (B,D) after indentation under a 0.245 N load. Cracks resulting from indentation are indicated by arrows. (A,B) Representative indents resulting in cracks with the length approximately equal to the mean crack diameter for the group, ×2200 magnification; (C,D) one of the longest cracks produced by indentation for each group, ×850 magnification.

after 11 weeks of exposure at a salinity of 30 and normocapnia). This reflects relatively small shell growth increments in oysters during this period (Fig. 1) compared with the overall variability in shell size and mass within experimental groups (data not shown). Salinity and $P_{CO_2}$ had no effect on total body mass or shell mass of juveniles under the conditions of this experiment (Table 2). In contrast, soft body mass decreased significantly under elevated $P_{CO_2}$ and low salinity conditions (Table 2, Fig. 2B). Overall, soft body mass was highest in juveniles maintained under control conditions of normocapnia and a salinity of 30 compared with all other groups (Fig. 2B).

### Mechanical properties of the shells

Vickers microhardness and fracture resistance of newly grown shells was significantly affected by interactions between salinity and $P_{CO_2}$, indicating that the effects of elevated $P_{CO_2}$ on shell mechanical properties differ depending on exposure salinity (Table 2, Fig. 2C). Elevated $P_{CO_2}$ did not affect the hardness of newly grown shells of juveniles kept at a salinity of 30, but led to a significant reduction of shell hardness at a salinity of 15 (Fig. 2C). Similarly, an increase in $P_{CO_2}$ had no effect on the crack radius (fracture resistance) at a salinity of 30, whereas at a salinity of 15 a trend towards longer crack radius was observed in shells of juveniles grown in hypercapnia compared with their normocapnic counterparts (Fig. 2D). Cracks resulting from indentations were considerably longer and more numerous in shells of juveniles held at low salinity and elevated $P_{CO_2}$ compared with those maintained under control conditions (Fig. 3). Overall, shells of juveniles held at a salinity of 15 and hypercapnia showed significantly lower hardness and fracture resistance than all other experimental groups.

### CA activity and mRNA expression

Specific activity of CA in the total body extracts was lower in juvenile oysters exposed to a salinity of 15 compared with those exposed to a salinity of 30 (Table 2, Fig. 4A). Elevated $P_{CO_2}$ had no significant effect on specific CA activity in whole-body extracts of juvenile oysters (Table 2, Fig. 4A). In contrast, expression of carbonic anhydrase mRNA was lower in juveniles exposed to elevated $P_{CO_2}$ and not significantly affected by salinity (Table 2, Fig. 4B).

Notably, the specific activity of CA was positively correlated with CA mRNA expression in juveniles maintained under normocapnia ($P_{CO_2}$ ~400 µatm); the correlation was significant at a salinity of 15 ($R$=0.895, $N$=5–7, $P$=0.04) and not significant at a salinity of 30 ($R$=0.709, $N$=7, $P$=0.07). In juveniles maintained under elevated $P_{CO_2}$ conditions, enzyme activity of CA was not significantly correlated with CA mRNA expression ($P$>0.05). When all experimental groups were considered together, correlation between CA activity and mRNA expression was not significant ($R$=–0.07, $N$=22, $P$=0.748).

### Energy-related indices

Exposure to lower salinity and/or elevated $P_{CO_2}$ had no effect on tissue levels of ATP in juvenile oysters (Table 2, Fig. 5A). In contrast, juveniles exposed to hypercapnia at a salinity of 15 had lower tissue levels of ADP and AMP compared with their counterparts maintained at a salinity of 15 and normocapnia (Fig. 5B,C). At a salinity of 30, $P_{CO_2}$ levels had no effect on tissue concentrations of ADP and AMP (Fig. 5B,C). Total concentrations of adenylates were not affected by salinity or $CO_2$ (Table 2), likely because the adenylate pool was dominated by ATP (with tissue ATP levels six to 10 times higher than those of ADP, and 40–186 times higher than those of AMP), and ATP levels did not change in response to exposure $P_{CO_2}$ and salinity.

At the same time, elevated $P_{CO_2}$ levels resulted in the partial depletion of tissue energy reserves (glycogen and lipids) in juveniles acclimated at a salinity of 30 (Fig. 5D,E). A similar trend to lower glycogen concentrations at elevated $P_{CO_2}$ was seen in

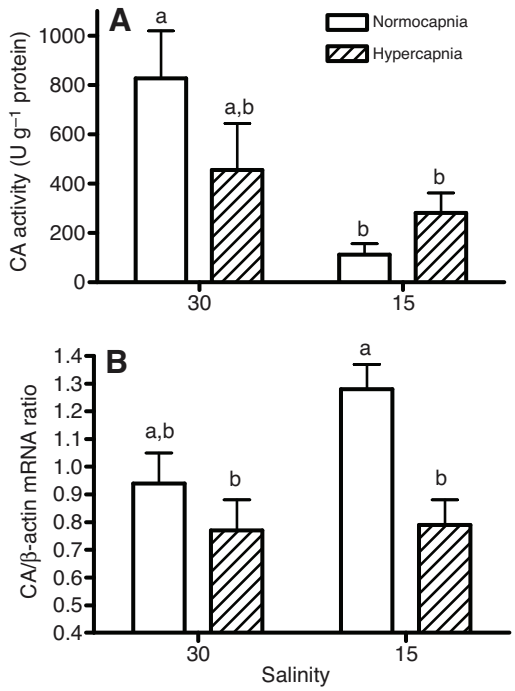


Fig. 4. Activity and mRNA expression of carbonic anhydrase (CA) in tissues of oyster juveniles maintained for 11 weeks in different salinities and $P_{CO_2}$ levels. (A) CA activity; (B) CA mRNA expression relative to mRNA expression of β-actin. CA mRNA expression was also normalized to 18S rRNA, yielding a pattern similar to that of the β-actin-normalized expression (data not shown). Within each graph, different letters indicate means that are significantly different from each other ($P$<0.05). If the columns share a letter, the respective means are not significantly different ($P$>0.05).

juveniles maintained at a salinity of 15, but it was not statistically significant (Fig. 5D). Elevated $P_{CO_2}$ had no significant effect on the lipid content of juveniles acclimated at a salinity of 15, but tissue lipid content was reduced in juveniles acclimated at a salinity of 15 compared with their counterparts acclimated at a salinity of 30 (Fig. 5E). Total protein content also tended to be lower in juveniles acclimated at a salinity of 15 compared with those acclimated at 30, but this trend was not statistically significant (Fig. 5F). Concentration of free glucose in tissues of oyster juveniles did not change in response to acclimation salinity or $P_{CO_2}$ (Table 2) and varied between 115 and 189 nmol g$^{-1}$ wet mass in all experimental groups.

### Metabolite profile

Tissue metabolite profile of the total body homogenates determined by the $^1$H-NMR spectra showed a significant shift in response to acclimation salinity (Table 2). At a salinity of 15, oyster juveniles contained significantly lower betaine, succinate and alanine levels and higher levels of lysine and acetate compared with their counterparts at a salinity of 30 (Fig. 6). Tissue levels of metabolites were not strongly affected by exposure $P_{CO_2}$, with the exception of acetate. At a salinity of 15, hypercapnia resulted in significantly lower acetate levels compared with those of normocapnic juveniles (Fig. 6D), whereas at a salinity of 30 no differences were observed between hypercapnic and normocapnic animals (Fig. 6A–E). Overall, tissue acetate levels in juveniles acclimated to normocapnia at a salinity of 15 were higher than in all other treatment groups in this study.

## DISCUSSION

Our study demonstrates that the effects of low salinity and elevated $P_{CO_2}$, alone and in combination, have overall negative effects on juvenile eastern oysters, based on observed mortalities and tissue growth rates. Individually, low salinity and hypercapnia affect measured traits in a distinctly different manner. Under the conditions of our experiment, low salinity is a greater single stressor than high $P_{CO_2}$, whereas the combination of these two factors produces greater changes in the physiology and shell properties of these mollusks than each of the factors alone (Table 3). This result may be explained by the exacerbation of seawater acidification and other changes in seawater chemistry by low salinity, such that both stressors synergistically affect similar mechanisms. In some cases (e.g. microhardness) the effects of low salinity and hypercapnia appear to be additive, whereas their combined effect on other parameters is more complex (Table 3). Overall, our data suggest that the

Table 3. Summary of the effects of salinity and $P_{CO_2}$ levels on the studied physiological and biomineralization traits in *C. virginica* juveniles

| Trait | High salinity/hypercapnia | Low salinity/normocapnia | Low salinity/hypercapnia |
|---|---|---|---|
| Mortality | ↑ | ↑↑↑ | ↑↑↑ |
| Body mass | ↓↓ | ↓↓ | ↓↓ |
| Vickers microhardness | = | = | ↓ |
| Crack length | = | = | ↑↑ |
| CA activity | = | ↓↓↓ | ↓↓ |
| CA mRNA | = | = | = |
| ATP | = | = | = |
| ADP | = | = | = |
| AMP | = | = | ↓↓↓ |
| Glycogen | ↓↓ | = | = |
| Lipids | ↓↓↓ | ↓↓↓ | ↓↓↓ |
| Proteins | = | = | = |
| Betaine | = | ↓↓↓ | ↓↓↓ |
| Acetate | = | ↑↑↑ | = |
| Lysine | = | ↑↑ | ↑↑ |
| Alanine | = | ↓↓ | ↓↓↓ |
| Succinate | = | ↓↓↓ | ↓↓↓ |

Arrows represent the direction of change (↑ and ↓ for an increase or decrease, respectively) for the trait values that differed significantly from the control group (maintained at a salinity of 30 and normocapnia), whereas number of signs in a cell represent the magnitude of a change. =, the respective differences were not statistically significant. Normocapnia and hypercapnia refer to $P_{CO_2}$ values of ~400 and ~700–800 μatm, respectively. High and low salinity refer to salinities of 30 and 15, respectively.

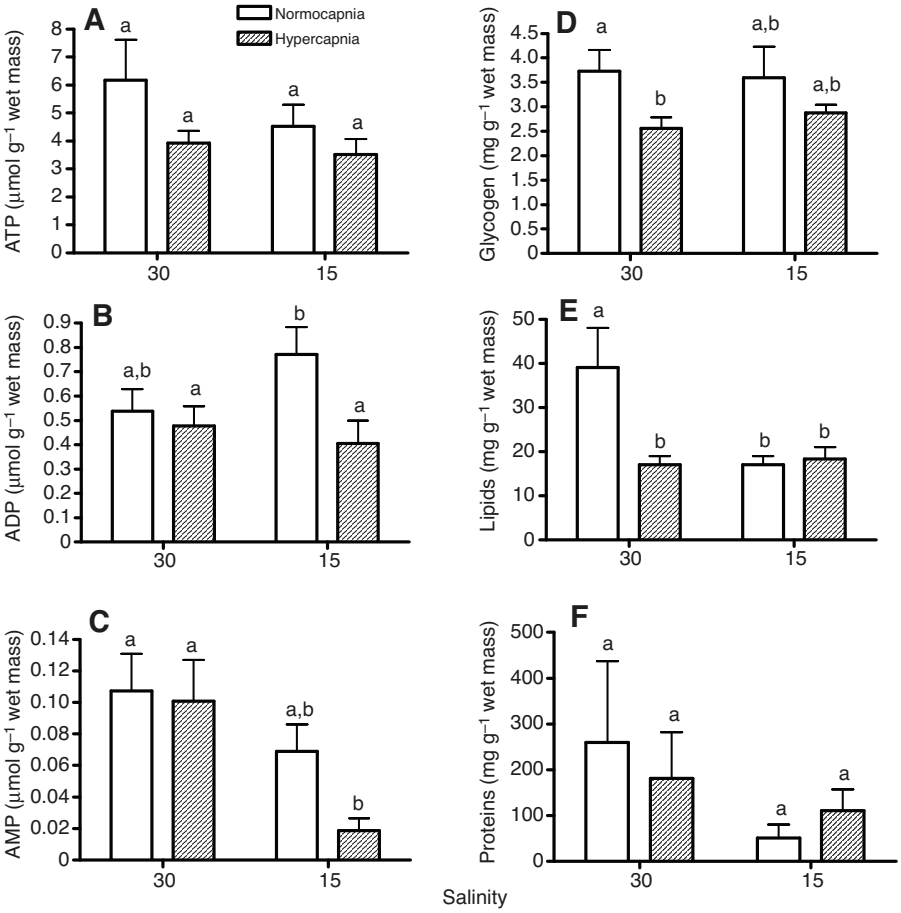


Fig. 5. Tissue concentrations of adenylates and major energy reserves in juveniles of the eastern oyster *C. virginica* maintained for 11 weeks in different salinities and $P_{CO_2}$ levels. Exposure conditions are given in Table 1. (A) ATP, (B) ADP, (C) AMP, (D) glycogen, (E) lipids and (F) proteins. Within each graph, different letters indicate means that are significantly different from each other ($P$<0.05). If the columns share a letter, the respective means are not significantly different ($P$>0.05).

predicted global increase in $CO_2$ levels would have a strong negative effect on coastal and estuarine populations of oysters. The magnitude of this impact can be modified by changes in environmental salinity such that low salinity sensitizes oyster juveniles to the negative impacts of $CO_2$-induced ocean acidification.

### Effects of $P_{CO_2}$ and salinity on juvenile growth and survival

Lowering seawater pH typically results in a reduction of growth in marine bivalves, with the degree of growth inhibition dependent on the magnitude of deviation in the environmental and/or body fluids pH from the organism's optimum (Ringwood and Keppler, 2002; Michaelidis et al., 2005b; Berge et al., 2006). A decrease in extracellular pH can cause metabolic depression and growth reduction; however, these effects are typically observed only during strong acidification [see Michaelidis et al., Pörtner, and Beniash et al., and references therein (Michaelidis et al., 2005b; Pörtner, 2008; Beniash et al., 2010)]. In oysters, no reduction in the metabolic rate was observed at $P_{CO_2}$ levels as high as 3500 µatm (Beniash et al., 2010). Metabolic studies are needed to investigate whether the negative tissue growth observed in oyster juveniles in response to hypercapnia in the present study involves metabolic rate depression.

Shell deposition rates decrease with increasing $P_{CO_2}$ in mollusks, and this change has been attributed to lower $CaCO_3$ saturation levels at the calcification site, which decreases the driving force for shell deposition and increases the dissolution of existing shell (Gazeau et al., 2007; Miller et al., 2009; Ries et al., 2009; Talmage and Gobler, 2009; Beniash et al., 2010; Talmage and Gobler, 2010). Reduced salinity also lowers water $CaCO_3$ saturation levels (Cai and Wang, 1998; Miller et al., 2009) and has been shown to lead to decreased growth rates in *C. virginica* and other mollusks (Almada-Villela, 1984; Paynter and Burreson, 1991; Nagarajan et al., 2006; Heilmayer et al., 2008). In addition, negative effects of low pH and/or salinity on the organism's energy budget may also contribute to diminished shell deposition rates (Almada-Villela, 1984; Michaelidis et al., 2005b; Nagarajan et al., 2006; Heilmayer et al., 2008; Beniash et al., 2010).

In this study, the total body mass and shell mass of juvenile oysters was not affected by exposure to different salinities and/or $P_{CO_2}$ levels. This may be due to the fact that new shell growth (as indicated by calcein growth marks; Fig. 1) was only a small fraction of the total shell volume for all exposure groups, including controls (normocapnia, salinity of 30), such that differences remain non-significant. Dry shell mass of the control group did not differ from that of the time zero (no exposure) group, indicating that the mass of the new growth region was not discernable within the context of variability among individual shell masses. In a previous study, Beniash et al. (Beniash et al., 2010) exposed younger juveniles (3 weeks post metamorphosis) of *C. virginica* to normocapnia (~390 µatm $P_{CO_2}$) and hypercapnia (~3500 µatm $P_{CO_2}$) for 20 weeks and reported substantial new growth as well as differences in shell mass between juveniles kept at different $P_{CO_2}$ levels. The discrepancy in the shell growth rates between the present study and the study by Beniash et al. (Beniash et al., 2010) likely reflects differences in the age of juveniles (7 *vs* 3 weeks post-metamorphosis, respectively), their size and the duration of experimental exposure (11 *vs* 20 weeks, respectively). In bivalves, the rate of shell growth decreases with increasing age and size (von Bertallanfy, 1964; Pauly, 2010), which would have been reflected in the slower shell

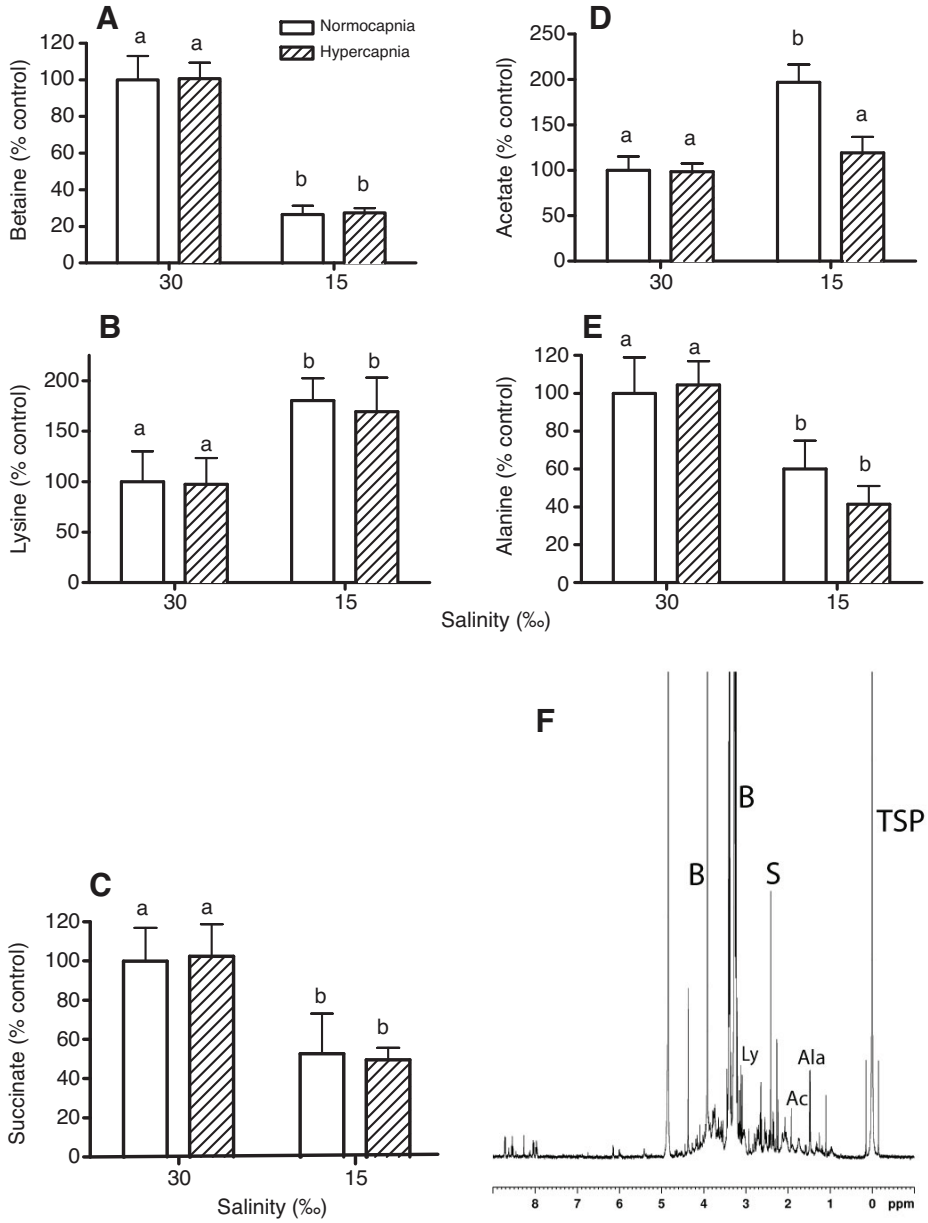


Fig. 6. Levels of tissue metabolites in juveniles of the eastern oyster *C. virginica* maintained for 11 weeks in different salinities and $P_{CO_2}$ levels. Exposure conditions are given in Table 1. (A) Betaine, (B) lysine, (C) succinate, (D) acetate and (E) alanine. Data, which are given in means ± s.e.m., are presented in % relative to control conditions (normocapnia, salinity of 30). Within each graph, different letters indicate means that are significantly different from each other ($P$<0.05). (F) A typical $^1$H-NMR spectrum obtained from a juvenile oyster under control conditions. Signals from analyzed metabolites are indicated: Ac, acetate; Ala, alanine; B, betaine; Ly, lysine; S, succinate; TMS, standard.

deposition rate in the older and larger juveniles used in this study. Here, we did not individually follow shell growth of the same juveniles throughout the experimental exposures and thus our growth estimates were based on the group size means. Given the relatively slow growth rate and considerable natural variation in size within a single age cohort of oysters (Collet et al., 1999; Bayne, 2000) (I.M.S., personal observation), the small growth increment was not detectable against the background of the natural size variation within the group. This technical limitation can be overcome in future studies by individually marking oysters and following changes in individual size and mass of their shells through time.

In contrast to shell mass, soft body mass was reduced in both low salinity groups and in the hypercapnic high salinity group, indicating negative growth (i.e. partial resorption of tissues). In control juveniles, the soft body mass did not significantly change during 11 weeks of exposure, consistent with the relatively slow growth rates discussed above. Previously, negative growth due to muscle wastage at low pH was found in a brittle star, *Amphiura filiformis*, while calcification rate was elevated to compensate for $CaCO_3$ dissolution (Wood et al., 2008). Elevated nitrogen excretion, indicative of protein breakdown expected during negative growth, was also found under low pH conditions (pH ~ 7.3) in the mussel *Mytilus edulis* (Michaelidis et al., 2005b). Notably, negative growth in juvenile oysters at low salinity and/or high $P_{CO_2}$ was associated with elevated mortality, indicating energy deficiency and supporting the notion that salinity and pH are among the key determinants of bivalve performance (including growth and survival) (Ringwood and Keppler, 2002; Heilmayer et al., 2008; Chapman et al., 2011).

A caveat, applicable not only to our growth rate estimates but to all physiological and biochemical traits reported in this study, is the fact that all traits were by necessity determined in those organisms that survived experimental treatments. Therefore, a survivor effect due to the differential mortality of organisms with different physiology or growth rates cannot be ruled out. Although the potential for such selective mortality is important to consider when interpreting the mechanisms of the observed physiological effects,

this effect will presumably also occur in the field. This would lead to similar shifts in physiological and biomineralization processes of the surviving population in response to elevated $P_{CO_2}$ and/or low salinity.

### Effects of $P_{CO_2}$ and salinity on the mechanical properties of the shells

Combined exposure to hypercapnia and low salinity significantly affected the mechanical properties of newly deposited shell in juvenile oysters. The portions of the shells deposited during combined exposure to hypercapnia and low salinity had significantly lower hardness and fracture resistance compared with other exposure groups. In addition, the shells of juveniles from the normocapnic low salinity treatment tended to have lower fracture resistance than the juveniles in the high salinity treatments, suggesting that salinity alone may also influence this parameter (possibly because of lower pH and/or other changes in seawater chemistry associated with low salinity seawater). Our results are consistent with mechanical testing of *C. virginica* shells by Beniash et al. (Beniash et al., 2010), which showed a significant decrease in hardness and fracture resistance of shells of juvenile oysters exposed to high $P_{CO_2}$ (~3500 μatm at a salinity of 30, $\Omega_{calcite}$=1.42). Similarly, elevated $P_{CO_2}$ resulted in the deposition of weaker, thinner and smaller shells in larvae of the California mussel, *Mytilus californianus* (Gaylord et al., 2011).

Earlier studies suggest that the differences in shell mechanical properties of oyster shell deposited under conditions of low pH and low calcite saturation are partially due to differences in shell ultrastructure (Beniash et al., 2010). The majority of *C. virginica* shell is composed of calcitic layers (laths) surrounded by an organic matrix (Carriker, 1996; Checa et al., 2007). The mechanical strength of multilayered materials such as bivalve shells is inversely related to the thickness of each layer (Anderson and Li, 1995; He et al., 1997). Thinner layers more frequently deflect cracks, hence forcing a more treacherous path and more interactions of the cracks with elastic organic material (Fratzl et al., 2007; Zhang et al., 2010). Using oyster juveniles, Beniash et al. (Beniash et al., 2010) showed that calcitic laths were significantly thicker in the shell deposited under low pH or low $\Omega_{calcite}$ conditions compared with that of oysters exposed to normocapnia. Altered ultrastructure in hypercapnia-exposed mollusks has also been shown in the developing nacre of *Pinctada fucata* (Welladsen et al., 2010) and at the growing edge of *Mercenaria mercenaria* and *Argopecten irradians* larvae (Talmage and Gobler, 2010). Further investigations, however, are needed to test this hypothesis as well as possible alternatives, such as changes in the shell organic and inorganic content and mineralogy. Irrespective of the exact mechanisms, compromised mechanical properties of the shell resulting from exposure to moderate hypercapnia and low salinity are likely to leave *C. virginica* more susceptible to predators and parasites.

### Effects of low salinity and hypercapnia on activity and expression of CA

Activity of CA, one of the key enzymes involved in carbonate chemistry regulation, acid–base homeostasis and biomineralization, was reduced during low salinity exposures in juvenile oysters, indicating a potential disturbance of biomineralization processes. CA facilitates the conversion of $CO_2$ into bicarbonate, supporting the maintenance of carbonate oversaturation and thus the driving force towards mineral deposition. It also supports pH regulation in both biomineralizing and non-biomineralizing tissues (Wilbur and Anderson, 1950; Wilbur and Jodrey, 1955; Nielsen and Frieden, 1972). Thus, a reduction in CA activity seen under the low salinity conditions could negatively affect shell growth and/or lead to acidosis, negatively affecting physiological processes including biomineralization, provided that activity becomes limiting for bicarbonate formation. Hypercapnia alone (~800 μatm) did not affect CA activity in juvenile oysters at high salinity.

Comparisons between the enzyme activity and mRNA expression for CA indicate that there is no consistent correlation between these two parameters across all treatment groups. This indicates that CA activity may be largely post-transcriptionally and/or post-translationally regulated. Another possible explanation for the lack of correlation between CA activity and mRNA levels could be the presence of multiple CA isoforms encoded by different genes, some of which were undetected by qRT-PCR but contributed to the total enzyme activity. Currently there is no evidence of multiple CA genes expressed in soft tissues of bivalves (Yu et al., 2006), but our knowledge about the genetic diversity of this enzyme in mollusks is very limited and requires further investigation. Overall, these data suggest that inferences about CA phenotype based on mRNA expression data should be interpreted with caution. Earlier studies in oysters and fish also showed poor correlation between enzyme activity and mRNA expression for several metabolic enzymes, including hexokinase, citrate synthase and cytochrome *c* oxidase (Lucassen et al., 2003; Ivanina et al., 2011). This suggests that, in aquatic ectotherms, enzyme activity may be a more reliable indicator of the metabolic phenotype than mRNA levels for several key metabolic and biomineralization enzymes.

### Effects of $P_{CO_2}$ and salinity on energy homeostasis of juvenile oysters

Exposure to moderate levels of environmental stress can lead to an increase in energy demand due to the energy costs of cellular protection systems, such as stress proteins and antioxidants, degradation and damage repair mechanisms, as well as active transport to maintain acid–base and ion homeostasis (Sokolova et al., 2011). These compensatory mechanisms allow successful acclimation to stress conditions, but can incur significant energy costs, disrupt energy homeostasis and affect cellular and whole-body energy status (Sokolova et al., 2011). Our study showed that exposure of *C. virginica* juveniles to low salinity and/or elevated $P_{CO_2}$ levels strongly affects their lipid and glycogen stores but does not affect the whole-body protein levels. This may reflect the fact that protein reserves in bivalves are typically used up only during extreme energy deficiency such as starvation (Baghdiguian and Riva, 1985; Albentosa et al., 2007). Hypercapnic exposure at a salinity of 30 led to a partial depletion of lipid and glycogen reserves in oyster juveniles (by 56 and 31%, respectively), indicating a mismatch between energy demand and supply. Hypercapnia also led to a ~20% decrease in whole-body glycogen content of juveniles exposed to hypercapnia at a salinity of 15 compared with their normocapnic counterparts; however, this decrease was not statistically significant. Earlier studies showed high energy demand (as indicated by elevated oxygen consumption rates) in juvenile *C. virginica* exposed to high $P_{CO_2}$ levels (~3500 μatm) (Beniash et al., 2010) as well as in adult *Crassostrea gigas* exposed to $P_{CO_2}$ levels of ~1000 μatm, although in the latter case the effect of $P_{CO_2}$ on respiration was only significant at elevated temperatures (Lannig et al., 2010). More severe $CO_2$-induced acidification (water pH 7.3) resulted in the reduction of metabolic rates in a mussel, *Mytilus galloprovincialis* (Michaelidis et al., 2005b). Thus, the change in basal metabolic demand in response to elevated $P_{CO_2}$ may be species-specific in bivalves and depend on the magnitude of the pH/$P_{CO_2}$ change in the environment and, consecutively, in body fluids.

In juveniles maintained at low salinity (15), whole-body lipid content was reduced by ~50% regardless of $P_{CO_2}$, compared with the normocapnic controls at a salinity of 30. These results indicate that exposure to low salinity may be associated with metabolic rearrangements that result in the preferential burning of lipids. Decrease of lipid stores in oyster juveniles kept at low salinity is consistent with earlier findings that low osmolarity changes the preferred fuel and strongly stimulates oxidation rates of acyl carnitines (C8–C18 fatty acid derivatives) in isolated oyster mitochondria (Ballantyne and Moyes, 1987b) while inhibiting glycolytic enzymes such as hexokinase and fructose biphosphatase (Ballantyne and Berges, 1991). Lysine concentrations were elevated by 70–80% in tissues of juveniles maintained in low salinity, consistent with the proposed high input of acetyl-CoA from lipid breakdown that may reduce the need for acetyl-CoA supply from lysine degradation. High acetyl-CoA production from the lipid oxidation may also explain the elevated acetate content in tissues of juvenile oysters kept at low salinity and normocapnia. Acetate accumulation in this group is unlikely to reflect an onset of partial anaerobiosis because no accumulation of succinate or alanine was observed (which typically precedes anaerobic acetate accumulation) (Michaelidis et al., 2005a; Kurochkin et al., 2009). Notably, no acetate accumulation was observed in juveniles maintained at low salinity and hypercapnia, possibly indicating high rates of mitochondrial acetate oxidation and/or slightly lower lipid degradation rates in this group. Alternatively, reduced lipid content and accumulation of acetate in the tissues of juvenile oysters maintained at low salinity may reflect reduced rates of lipid biosynthesis. The effects of salinity on lipid biosynthesis of mollusks are not known. Studies in marine crabs, however, showed that exposure to reduced salinity either strongly enhanced (in *Callinectus sapidus*) or had no significant effect on lipid biosynthesis (in *Libinia emarginata*) (Whitney, 1974). Thus, inhibition of lipid biosynthesis appears to be a less likely explanation of the reduced lipid content in oysters maintained under low salinity conditions.

Acclimation to low salinity led to a shift in the metabolic profile in oysters, notably to a strong reduction in the levels of betaine and alanine (by approximately 70 and 40%, respectively), consistent with their role as major osmolytes in bivalves (Powell et al., 1982; Neufeld and Wright, 1996; Hosoi et al., 2003). In contrast, elevated $P_{CO_2}$ had no effect on the metabolite profile in whole bodies of oyster juveniles in this study except for the lower acetate content of tissues from hypercapnic juveniles compared with their normocapnic counterparts at a salinity of 15. This change, however, reflects elevated acetate levels in the juveniles maintained under normocapnia and low salinity conditions rather than acetate depletion in the hypercapnic group. No anaerobic end products (alanine, succinate or acetate) were accumulated under elevated $P_{CO_2}$, indicating that the juveniles were capable of fully maintaining their metabolic demand with aerobic pathways.

Juvenile oysters were capable of maintaining normal steady-state levels of ATP in all experimental treatments, suggesting that the metabolic adjustments to low salinity and elevated $P_{CO_2}$ are sufficient to prevent ATP depletion and severe cellular energy deficiency. This is consistent with earlier studies that have shown that intertidal mollusks including oysters effectively defend the cellular ATP pool, so that ATP depletion occurs only under conditions of severe energy limitation such as prolonged anoxia (Hochachka and Guppy, 1987; Sukhotin and Pörtner, 1999; Sokolova et al., 2000; Kurochkin et al., 2008). ADP levels were significantly elevated in juveniles from the low salinity normocapnic group, and AMP levels were reduced in juveniles kept at low salinity and hypercapnia. These changes may be indicative of higher metabolic flux and thus metabolic rate in these groups, which is typically supported by elevated ADP/ATP ratios (Pörtner et al., 1998; Hardie and Hawley, 2001; Ivanina et al., 2010); however, further investigations are required to test this hypothesis. Although cellular ATP content was not significantly affected by salinity and $CO_2$ levels, a decline in the carbon energy stores went hand-in-hand with the negative growth and elevated mortality of juveniles exposed to hypercapnia and/or low salinity. This suggests that the tissue stores of fermentable substrates may be a more sensitive indicator of long-term energy deficit compared with ATP levels that are tightly regulated to ensure cellular survival (Pörtner, 1993; Pörtner et al., 1996).

## Conclusions

Reduced salinity and elevated $P_{CO_2}$ levels interactively affect survival, growth, energy status and shell mechanical properties in juvenile oysters. Low salinity can strongly modify the negative effects of high $P_{CO_2}$/low pH on the shell's material properties, weakening shells of the juveniles and making them more prone to predators, parasites and other mechanical damages. Hypercapnia and low salinity, either alone or in combination, also led to a reduction in tissue growth and survival of juveniles, possibly because of energy limitation in the stressed state, as indicated by the partial depletion of tissue energy stores. Such energy limitations can affect the organism's fitness and general stress tolerance and are likely to translate into reduced survival, growth and reproduction of oysters (Pörtner, 2008; Sokolova et al., 2011). The observed effects of hypercapnia and salinity stress on oyster physiology and the shell's material properties are especially remarkable given that oysters, like most estuarine species, can be exposed to periodical bouts of extreme $P_{CO_2}$ levels in their habitats with a reduction in seawater pH down to 6.0–7.5 (Pritchard, 1967; Burnett, 1997; Ringwood and Keppler, 2002) and thus are often considered hypercapnia tolerant. Overall, this study suggests that long-term exposure to a modest (by estuarine standards) increase in $P_{CO_2}$, as predicted with global climate change in the next century, will likely have negative consequences on survival and performance of oysters, especially when combined with low salinity stress in estuaries.

## ACKNOWLEDGEMENTS

We would like to thank R. M. Wittig for his support of NMR analysis.

## FUNDING

This work was supported by funds provided by the National Science Foundation [award IOS-0951079 to I.M.S. and E.B.], UNC Charlotte Faculty Research Grant [to I.M.S.], and the 'Polar regions and coasts in a changing Earth system' (PACES) research program of the Alfred Wegener Institute.

## REFERENCES

**Albentosa, M., Fernandez-Reiriz, M. J., Labarta, U. and Perez-Camacho, A.** (2007). Response of two species of clams, *Ruditapes decussatus* and *Venerupis pullastra*, to starvation: Physiological and biochemical parameters. *Comp. Biochem. Physiol.* **146B**, 241-249.

**Almada-Villela, P. C.** (1984). The effects of reduced salinity on the shell growth of small *Mytilus edulis*. *J. Mar. Biol. Assoc. UK* **64**, 171-182.

**Anderson, P. M. and Li, C.** (1995). Hall-petch relations for multilayered materials. *Nanostruct. Mater.* **5**, 349-362.

**Anstis, G. R., Chantikul, P., Lawn, B. R. and Marshall, D. B.** (1981). A critical evaluation of indentation techniques for measuring fracture toughness: I. Direct crack measurements. *J. Am. Ceram. Soc.* **64**, 533-538.

**Baghdiguian, S. and Riva, A.** (1985). Metabolic modifications brought by the synergic action of cadmium and experimental starvation of clams *Ruditapes decussatus*. *Mar. Environ. Res.* **17**, 289.

**Baldassarri, M., Margolis, H. C. and Beniash, E.** (2008). Compositional determinants of mechanical properties of enamel. *J. Dent. Res.* **87**, 645-649.

**Ballantyne, J. S. and Berges, J. A.** (1991). Enzyme activities of gill, hepatopancreas, mantle and adductor muscle of the oyster (*Crassostrea virginica*) after changes in diet and salinity. *Can. J. Fish. Aquat. Sci.* **48**, 1117-1123.

**Ballantyne, J. S. and Moyes, C. D.** (1987a). The effects of salinity acclimation on the osmotic properties of mitochondria from the gill of *Crassostrea virginica. J. Exp. Biol.* **133**, 449-456.

**Ballantyne, J. S. and Moyes, C. D.** (1987b). Osmotic effects on fatty acid, pyruvate, and ketone body oxidation in oyster gill mitochondria. *Physiol. Zool.* **60**, 713-721.

**Bayne, B. L.** (2000). Relations between variable rates of growth, metabolic costs and growth efficiencies in individual Sydney rock oysters (*Saccostrea commercialis*). *J. Exp. Mar. Biol. Ecol.* **251**, 185-203.

**Beniash, E., Ivanina, A., Lieb, N. S. and Kurochkin, I. I. M. S.** (2010). Elevated levels of carbon dioxide affect metabolism and shell formation in oysters *Crassostrea virginica. Mar. Ecol. Prog. Ser.* **419**, 95-108.

**Berge, J. A., Bjerkeng, B., Pettersen, O., Schaanning, M. T. and Øxnevad, S.** (2006). Effects of increased sea water concentrations of $CO_2$ on growth of the bivalve *Mytilus edulis* L. *Chemosphere* **62**, 681-687.

**Berger, V. J.** (1986). *Adaptations of Marine Molluscs to Changes of Environmental Salinity.* Leningrad: Nauka.

**Berger, V. J. and Kharazova, A. D.** (1997). Mechanisms of salinity adaptations in marine molluscs. *Hydrobiologia* **355**, 115-126.

**Bergmeyer, H. U.** (1985). *Methods of Enzymatic Analysis. Vol VI. Metabolites 1, Carbohydrates.* Weinheim, Germany: VCH Verlagsgesellschaft.

**Burnett, L. E.** (1997). The challenges of living in hypoxic and hypercapnic aquatic environments. *Am. Zool.* **37**, 633-640.

**Byrne, M., Ho, M., Wong, E., Soars, N. A., Selvakumaraswamy, P., Shepard-Brennand, H., Dworjanyn, S. A. and Davis, A. R.** (2010). Unshelled abalone and corrupted urchins: development of marine calcifiers in a changing ocean. *Proc. R. Soc. Lond. B* **278**, 2376-2383.

**Cai, W. J. and Wang, Y.** (1998). The chemistry, fluxes, and sources of carbon dioxide in the estuarine waters of the Satilla and Altamaha Rivers, Georgia. *Limnol. Oceanogr.* **43**, 657-668.

**Carriker, M. R.** (1996). The shell and ligament. In *The Eastern Oyster Crassostrea virginica* (ed. V. S. Kennedy, R. I. E. Newell and A. F. Able), pp. 75-168. College Park, MD: Maryland Sea Grant College.

**Chapman, R. W., Mancia, A., Beal, M., Veloso, A., Rathburn, C., Blair, A., Holland, A. F., Warr, G. W., Didinato, G. U. Y., Sokolova, I. M. et al.** (2011). The transcriptomic responses of the eastern oyster, *Crassostrea virginica*, to environmental conditions. *Mol. Ecol.* **20**, 1431-1449.

**Checa, A. G., Esteban-Delgado, F. J. and Rodriguez-Navarro, A. B.** (2007). Crystallographic structure of the foliated calcite of bivalves. *J. Struct. Biol.* **157**, 393-402.

**Checa, A. G., Esteban-Delgado, F. J., Ramírez-Rico, J. and Rodríguez-Navarro, A. B.** (2009). Crystallographic reorganization of the calcitic prismatic layer of oysters. *J. Struct. Biol.* **167**, 261-270.

**Collet, B., Boudry, P., Thebault, A., Heurtebise, S., Morand, B. and Gerard, A.** (1999). Relationship between pre- and post-metamorphic growth in the Pacific oyster *Crassostrea gigas* (Thunberg). *Aquaculture* **175**, 215-226.

**Crenshaw, M. A.** (1972). The inorganic composition of molluscan extrapallial fluid. *Biol. Bull.* **143**, 506-513.

**Davenport, J.** (1985). Osmotic control in marine invertebrates. In *Physiological Adaptations of Marine Animals. Symposia of the Society for Experimental Biology* (ed. M. S. Laverack), pp. 207-244. Cambridge: The Company of Biologists.

**Day, E. G., Branch, G. M. and Viljoen, C.** (2000). How costly is molluscan shell erosion? A comparison of two patellid limpets with contrasting shell structures. *J. Exp. Mar. Biol. Ecol.* **243**, 185-208.

**Denman, K., Christian, J. R., Steiner, N., Pörtner, H-O. and Nojiri, Y.** (2011). Potential impacts of future ocean acidification on marine ecosystems and fisheries: current knowledge and recommendations for future research. ICES *J. Mar. Sci.* **68**, 1019-1029.

**Dickson, A. G.** (1990). Standard potential of the reaction: AgCl(s) + 1/2 $H_2$(g) = Ag(s) + HCl(aq), and the standard acidity constant of the ion $HSO_4^-$ in synthetic seawater from 273.15 to 318.15 K. *J. Chem. Thermodyn.* **22**, 113-127.

**Dickson, A. G., Sabine, C. L. and Christian, J. R.** (2007). Guide to best practices for ocean $CO_2$ measurements. *PICES Spec. Publ.* **3**, 191 pp.

**Digby, P. S. B.** (1968). The mechanism of calcification in the molluscan shell. In *Symposium of Zoological Society of London. Studies in the Structure, Physiology and Ecology of Molluscs* (ed. V. Fretter), pp. 93-107. London: Academic Press.

**Doney, S. C., Fabry, V. J., Feely, R. A. and Kleypas, J. A.** (2009). Ocean acidification: the other $CO_2$ problem. *Annu. Rev. Mar. Sci.* **1**, 169-192.

**Folch, J., Lees, M. and Stanley, G. H. S.** (1957). A simple method for the isolation and purification of total lipids from animal tissues. *J. Biol. Chem.* **226**, 497-509.

**Fratzl, P., Gupta, H. S., Fischer, F. D. and Kolednik, O.** (2007). Hindered crack propagation in materials with periodically varying Young's modulus – lessons from biological materials. *Adv. Mater.* **19**, 2657-2661.

**Furuhashi, T., Schwarzinger, C., Miksik, I., Smrz, M. and Beran, A.** (2009). Molluscan shell evolution with review of shell calcification hypothesis. *Comp. Biochem. Physiol.* **154B**, 351-371.

**Gambhir, K. K., Ornasir, J., Verle, H. and Bonar, A.** (2007). Decreased total carbonic anhydrase esterase activity and decreased levels of carbonic anhydrase 1 isozyme in erythocytes of type II diabetic patients. *Biochem. Genet.* **45**, 431-439.

**Gaylord, B., Hill, T. M., Sanford, E., Lenz, E. A., Jacobs, L. A., Sato, K. N., Russell, A. D. and Hettinger, A.** (2011). Functional impacts of ocean acidification in an ecologically critical foundation species. *J. Exp. Biol.* **214**, 2586-2594.

**Gazeau, F., Quiblier, C., Jansen, J. M., Gattuso, J. P., Middelburg, J. J. and Heip, C. H. R.** (2007). Impact of elevated $CO_2$ on shellfish calcification. *Geophys. Res. Lett.* **34**, L07603.

**Geller, J. B.** (1990). Consequences of a morphological defense: growth, repair and reproduction by thin-and thick-shelled morphs of *Nucella emarginata* (Deshayes) (Gastropoda: Prosobranchia). *J. Exp. Mar. Biol. Ecol.* **144**, 173-184.

**Gooding, R. A., Harley, C. D. G. and Tang, E.** (2009). Elevated water temperature and carbon dioxide concentration increase the growth of a keystone echinoderm. *Proc. Natl. Acad. Sci. USA* **106**, 9316-9321.

**Grieshaber, M., Kronig, E. and Koormann, R.** (1978). A photometric estimation of phospho-L-arginine, arginine and octopine using homogeneous octopine dehydrogenase isozyme 2 from the squid, *Loligo vulgaris* Lam. *Hoppe Seylers Z. Physiol. Chem.* **359**, 133-136.

**Hardie, D. G. and Hawley, S. A.** (2001). AMP-activated protein kinase: the energy charge hypothesis revisited. *BioEssays* **23**, 1112-1119.

**Hawkins, A. J. S. and Hilbish, T. J.** (1992). The costs of cell volume regulation: protein metabolism during hyperosmotic adjustment. *J. Mar. Biol. Assoc. UK* **72**, 569-578.

**He, J. L., Li, W. Z. and Li, H. D.** (1997). Simulation of nacre with TiN/Pt multilayers and a study of their hardness. *J. Mater. Res.* **12**, 3140-3145.

**Heilmayer, O., Honnen, C., Jacob, U., Chiantore, M., Cattaneo-Vietti, R. and Brey, T.** (2005). Temperature effects on summer growth rates in the Antarctic scallop, *Adamussium colbecki. Polar Biol.* **28**, 523-527.

**Heilmayer, O., Digialleonardo, J., Qian, L. and Roesijadi, G.** (2008). Stress tolerance of a subtropical *Crassostrea virginica* population to the combined effects of temperature and salinity. *Estuar. Coast. Shelf Sci.* **79**, 179-185.

**Hochachka, P. W. and Guppy, M.** (1987). *Metabolic Arrest and the Control of Biological Time.* Cambridge, MA: Harvard University Press.

**Hofmann, A. F., Middelburg, J. J., Soetaert, K. and Meysman, F. J. R.** (2009). pH modelling in aquatic systems with time-variable acid-base dissociation constants applied to the turbid, tidal Scheldt estuary. *Biogeosciences* **6**, 1539-1561.

**Hosoi, M., Kubota, S., Toyohara, M., Toyohara, H. and Hayashi, I.** (2003). Effect of salinity change on free amino acid content in Pacific oyster. *Fish. Sci.* **69**, 395-400.

**Ivanina, A. V., Sokolov, E. P. and Sokolova, I. M.** (2010). Effects of cadmium on anaerobic energy metabolism and mRNA expression during air exposure and recovery of an intertidal mollusk *Crassostrea virginica. Aquat. Toxicol.* **99**, 330-342.

**Ivanina, A. V., Froelich, B., Williams, T., Sokolov, E. P., Oliver, J. D. and Sokolova, I. M.** (2011). Interactive effects of cadmium and hypoxia on metabolic responses and bacterial loads of eastern oysters *Crassostrea virginica* Gmelin. *Chemosphere* **82**, 377-389.

**Iverson, S. J., Lang, S. L. and Cooper, M. H.** (2001). Comparison of the Bligh and Dyer and Folch methods for total lipid determination in a broad range of marine tissue. *Lipids* **36**, 1283-1287.

**Kaehler, S. and McQuaid, C. D.** (1999). Use of the fluorochrome calcein as an *in situ* growth marker in the brown mussel *Perna perna. Mar. Biol.* **133**, 455-460.

**Kennedy, V. S., Newell, R. I. E. and Eble, A. F.** (1996). *The Eastern Oyster Crassostrea virginica.* College Park, MD: Maryland Sea Grant.

**Keppler, D. and Decker, K.** (1984). Glycogen. In *Methods of Enzymatic Analysis* (ed. H. U. Bergmeyer), pp. 11-18. Weinheim: Verlag Chemie.

**Kinne, O.** (1971). Salinity: animals: invertebrates. In *Marine Ecology,* Vol. 1 (ed. O. Kinne), pp. 821-996. New York: Wiley.

**Kleypas, J. A., Feely, R. A., Fabry, V. J., Langdon, C., Sabine, C. L. and Robbins, L. L.** (2006). *Impacts of Ocean Acidification on Coral Reefs and Other Marine Calcifiers. A Guide for Future Research.* Report of a workshop held 18-20 April 2005, St Petersburg, FL, sponsored by NSF, NOAA and the US Geological Survey, 88 pp.

**Kurochkin, I., Ivanina, A., Eilers, S. and Sokolova, I.** (2008). Effects of environmental anoxia and re-oxygenation on mitochondrial function and metabolism of eastern oysters (*Crassostrea virginica). Comp. Biochem. Physiol.* **150A**, S161.

**Kurochkin, I. O., Ivanina, A. V., Eilers, S., Downs, C. A., May, L. A. and Sokolova, I. M.** (2009). Cadmium affects metabolic responses to prolonged anoxia and reoxygenation in eastern oysters *Crassostrea virginica. Am. J. Physiol. Regul. Integr. Comp. Physiol.* **297**, R1262-R1272.

**Lannig, G., Eilers, S., Pörtner, H. O., Sokolova, I. M. and Bock, C.** (2010). Impact of ocean acidification on energy metabolism of oyster, *Crassostrea gigas* – changes in metabolic pathways and thermal response. *Mar. Drugs* **8**, 2318-2339.

**Lewis, E. and Wallace, D. W. R.** (1998). *Program Developed for $CO_2$ System Calculations. ORNL/CDIAC-105.* Oak Ridge, TN: Carbon Dioxide Information Analysis Center, Oak Ridge National Laboratory, US Department of Energy.

**Lucassen, M., Schmidt, A., Eckerle, L. G. and Pörtner, H.-O.** (2003). Mitochondrial proliferation in the permanent vs. temporary cold: enzyme activities and mRNA levels in Antarctic and temperate zoarcid fish. *Am. J. Physiol. Regul. Integr. Comp. Physiol.* **285**, R1410-R1420.

**Malheiro, A., Gambhir, K., Bland, G., Abrams, C., Headings, V. and Abdul-Rahman, M.** (2009). Erythrocyte total carbonic anhydrase esterase activity in African American obese children: reduction starts at a young age. *Biochem. Genet.* **47**, 322-328.

**Michaelidis, B., Haas, D. and Grieshaber, M. K.** (2005a). Extracellular and intracellular acid-base status with regard to the energy metabolism in the oyster *Crassostrea gigas* during exposure to air. *Physiol. Biochem. Zool.* **78**, 373-383.

**Michaelidis, B., Ouzounis, C., Paleras, A. and Pörtner, H. O.** (2005b). Effects of long-term moderate hypercapnia on acid–base balance and growth rate in marine mussels *Mytilus galloprovincialis. Mar. Ecol. Prog. Ser.* **293**, 109-118.

**Miller, A. W., Reynolds, A. C., Sobrino, C. and Riedel, G. F.** (2009). Shellfish face uncertain future in high $CO_2$ world: influence of acidification on oyster larvae calcification and growth in estuaries. *PLoS ONE* **4,** e5661.

**Millero, F. J., Graham, T. B., Huang, F., Bustos-Serrano, H. and Pierrot, D.** (2006). Dissociation constants of carbonic acid in seawater as a function of salinity and temperature . *Mar. Chem.* **100**, 80-94.

**Mook, W. G. and Koene, B. K. S.** (1975). Chemistry of dissolved inorganic carbon in estuarine and coastal brackish waters. *Estuar. Coast. Mar. Sci.* **3**, 325-336.

**Nagarajan, R., Lea, S. E. G. and Goss-Custard, J. D.** (2006). Seasonal variations in mussel, *Mytilus edulis* L. shell thickness and strength and their ecological implications. *J. Exp. Mar. Biol. Ecol.* **339**, 241-250.

**Neufeld, D. S. and Wright, S. H.** (1996). Response of cell volume in *Mytilus* gill to acute salinity change. *J. Exp. Biol.* **199**, 473-484.

**Nielsen, S. A. and Frieden, E.** (1972). Carbonic anhydrase activity in molluscs. *Comp. Biochem. Physiol.* **41B**, 461-468.
**Palmer, A. R.** (1983). Relative cost of producing skeletal organic matrix versus calcification: evidence from marine gastropods. *Mar. Biol.* **75**, 287-292.
**Palmer, A. R.** (1992). Calcification in marine molluscs: how costly is it? *Proc. Natl. Acad. Sci. USA* **89**, 1379-1382.
**Pauly, D.** (2010). Gasping fish and panting squids: oxygen, temperature and the growth of water-breathing animals. In *Excellence in Ecology* (ed. O. Kinne), Book 22. Oldendorf/Luhe, Germany: International Ecology Institute Publications.
**Paynter, K. T. and Burreson, E. M.** (1991). Effects of *Perkinsus marinus* infection in the eastern oyster, *Crassostrea virginica*: II. Disease development and impact on growth rate at different salinities. *J. Shellfish Res.* **10**, 425-431.
**Pfaffl, M. W.** (2001). A new mathematical model for relative quantification in real-time RT-PCR. *Nucleic Acids Res.* **29**, 2002-2007.
**Pörtner, H. O.** (1987). Contributions of anaerobic metabolism to pH regulation in animal tissues: theory. *J. Exp. Biol.* **131**, 69-87.
**Pörtner, H. O.** (1993). Multicompartmental analyses of acid-base and metabolic homeostasis during anaerobiosis: Invertebrate and lower vertebrate examples. In *Surviving Hypoxia: Mechanisms of Control and Adaptation* (ed. P. W. Hochachka, P. L. Lutz, T. Sick, M. Rosental and G. van den Thillart), pp. 139-156. Boca Raton, FL: CRC Press.
**Pörtner, H.** (2008). Ecosystem effects of ocean acidification in times of ocean warming: a physiologist's view. *Mar. Ecol. Prog. Ser.* **373**, 203-217.
**Pörtner, H.-O.** (2010). Oxygen- and capacity-limitation of thermal tolerance: a matrix for integrating climate-related stressor effects in marine ecosystems. *J. Exp. Biol.* **213**, 881-893.
**Pörtner, H. O. and Bock, C.** (2000). A contribution of acid-base regulation to metabolic depression in marine ectotherms. In *Life in the Cold* (ed. G. Heldmaier and M. Klingenspor), pp. 443-458. Berlin: Springer Verlag.
**Pörtner, H. O., Finke, E. and Lee, P. G.** (1996). Metabolic and energy correlates of intracellulr pH in progressive fatigue of squid (*L. brevis*) mantle muscle. *Am. J. Physiol.* **271**, R1403-R1414.
**Pörtner, H. O., Reipschläger, A. and Heisler, N.** (1998). Acid–base regulation, metabolism and energetics in *Sipunculus nudis* as a function of ambient carbon dioxide level. *J. Exp. Biol.* **201**, 43-55.
**Powell, E. N., Kasschau, M., Chen, E., Koenig, M. and Pecon, J.** (1982). Changes in the free amino acid pool during environmental stress in the gill tissue of the oyster, Crassostrea virginica. *Comp. Biochem. Physiol.* **71A**, 591-598.
**Pritchard, D. W.** (1967). What is an estuary: physical viewpoint. In *Estuaries* (ed. G. H. Lauff), pp. 3-5. Washington, DC: American Association for the Advancement of Science.
**Prosser, C. L.** (1973). *Comparative Animal Physiology, Vol. I. Environmental Physiology.* Philadelphia, London, Toronto: W. B. Saunders Company.
**Riascos, J., Guzman, N., Laudien, J., Helmayer, O. and Oliva, M.** (2007). Suitability of three stains to mark shells of *Concholepas concholepas* (Gastropoda) and *Mesodesma donacium* (Bivalvia). *J. Shellfish Res.* **26**, 43-49.
**Riebesell, U., Fabry, V. J., Hansson, L. and Gattuso, J.-P.** (2010). *EPOCA: Guide to Best Practices for Ocean Acidification Research and Data Reporting.* Luxembourg: Publications Office of the European Union.
**Ries, J. B., Cohen, A. L. and McCorkle, D. C.** (2009). Marine calcifiers exhibit mixed responses to $CO_2$-induced ocean acidification. *Geology* **37**, 1131-1134.
**Ringwood, A. H. and Keppler, C. J.** (2002). Water quality variation and clam growth: is pH really a non-tissue in estuaries. *Estuaries* **25**, 901-907.
**Sanni, B., Williams, K., Sokolov, E. P. and Sokolova, I. M.** (2008). Effects of acclimation temperature and cadmium exposure on mitochondrial aconitase and LON protease from a model marine ectotherm, *Crassostrea virginica*. *Comp. Biochem. Physiol.* **147C**,101-112.
**Smeda, J. S. and Houston, A. H.** (1979). Carbonic anhydrase (acetazolamide-sensitive esterase) activity in the red blood cells of thermally acclimated rainbow trout, *Salmo gairdneri*. *Comp. Biochem. Physiol.* **62A**, 719-723.
**Sokolova, I. M., Bock, C. and Pörtner, H. O.** (2000). Resistance to freshwater exposure in White Sea *Littorina* spp. I: Anaerobic metabolism and energetics. *J. Comp. Physiol. B* **170**, 91-103.
**Sokolova, I. M., Sukhotin, A. A. and Lannig, G.** (2011). Stress effects on metabolism and energy budgets in mollusks. In *Oxidative Stress in Aquatic Ecosystems* (ed. D. Abele, J. P. Vazquez-Medina and T. Zenteno-Savin), pp. 263-280. Boston: Wiley Blackwell.
**Sukhotin, A. A. and Pörtner, H. O.** (1999). Habitat as a factor involved in the physiological response to environmental anaerobiosis of White Sea *Mytilus edulis*. *Mar. Ecol. Prog. Ser.* **184**, 149-160.
**Talmage, S. C. and Gobler, C. J.** (2009). The effects of elevated carbon dioxide concentrations on the metamorphosis, size, and survival of larval hard clams (*Mercenaria mercenaria*), bay scallops (*Argopecten irradians*), and eastern oysters (*Crassostrea virginica*) *Limnol. Oceanogr.* **54**, 2072-2080.
**Talmage, S. C. and Gobler, C. J.** (2010). Effects of past, present, and future ocean carbon dioxide concentrations on the growth and survival of larval shellfish. *Proc. Natl. Acad. Sci. USA* **107**, 17246-17251.
**Truchot, J. P.** (1988). Problems of acid–base balance in rapidly changing intertidal environments. *Am. Zool.* **28**, 55-64.
**von Bertallanfy, L.** (1964). Basic concepts in quantitative biology of metabolism. *Helgol. Wiss. Meeresunters.* **9**, 5-37.
**Waldbusser, G., Voigt, E., Bergschneider, H., Green, M. and Newell, R.** (2011). Biocalcification in the eastern oyster (*Crassostrea virginica*) in relation to long-term trends in Chesapeake Bay pH. *Estuar. Coasts* **34**, 221-231.
**Welladsen, H. M., Southgate, P. C. and Heimann, K.** (2010). The effects of exposure to near-future levels of ocean acidification on shell characteristics of *Pinctada fucata* (Bivalvia: Pteriidae). *Molluscan Res.* **30**, 125-130.
**Wheeler, A. P.** (1992). Mechanisms of molluscan shell formation. In *Calcification in Biological Systems* (ed. E. Bonucci), pp. 179-121. Boca Raton, FL: CRC Press.
**Whitney, J. O.** (1974). The effect of external salinity upon lipid synthesis in the blue crab *Callinectes sapidus* rathbun and in the spider crab *Libinia em arginata* leech. *Comp. Biochem. Physiol.* **49A**, 433-440.
**Wilbur, K. M. and Anderson, N. G.** (1948). Electrometric and colometric determination of carbonic anhydrase. *J. Biol. Chem.* **176**, 147-154.
**Wilbur, K. M. and Anderson, N. G.** (1950). Carbonic anhydrase and growth in the oyster and *Busycon*. *Biol. Bull.* **98**, 19-24.
**Wilbur, K. M. and Jodrey, L. H.** (1955). Studies on shell formation. V. The inhibition of shell formation by carbonic anhydrase inhibitors. *Biol. Bull.* **108**, 359-365.
**Wood, H. L., Spicer, J. I. and Widdicombe, S.** (2008). Ocean acidification may increase calcification rates, but at a cost. *Proc. R. Soc. Lond. B* **275**,1767-1773.
**Wood, H., Spicer, J., Lowe, D. and Widdicombe, S.** (2010). Interaction of ocean acidification and temperature; the high cost of survival in the brittlestar *Ophiura ophiura*. *Mar. Biol.* **157**, 2001-2013.
**Yu, Z., Xie, L., Lee, S. and Zhang, R.** (2006). A novel carbonic anhydrase from the mantle of the pearl oyster (Pinctada fucata). *Comp. Biochem. Physiol.* **143B**, 190-194.
**Zeebe, R. E. and Wolf-Gladrow, D.** (2001). $CO_2$ in seawater: equilibrium, kinetics, isotopes. *Oceanography Series* **65**, 1-341.
**Zhang, J. Y., Liu, G., Zhang, X., Zhang, G. J., Sun, J. and Ma, E.** (2010). A maximum in ductility and fracture toughness in nanostructured Cu/Cr multilayer films. *Scripta Materialia* **62**, 333-336.